



Article

Functional Characterization of TetR-like Transcriptional Regulator PA3973 from *Pseudomonas aeruginosa*

Karolina Kotecka , Adam Kawalek , Magdalena Modrzejewska-Balcerek, Jan Gawor, Karolina Zuchniewicz, Robert Gromadka and Aneta Agnieszka Bartosik *

Institute of Biochemistry and Biophysics, Polish Academy of Sciences, Pawinskiego 5a, 02-106 Warsaw, Poland

* Correspondence: anetab2@ibb.waw.pl

Abstract: *Pseudomonas aeruginosa*, a human opportunistic pathogen, is a common cause of nosocomial infections. Its ability to survive under different conditions relies on a complex regulatory network engaging transcriptional regulators controlling metabolic pathways and capabilities to efficiently use the available resources. *P. aeruginosa* PA3973 encodes an uncharacterized TetR family transcriptional regulator. In this study, we applied a transcriptome profiling (RNA-seq), genome-wide identification of binding sites using ChIP-seq, as well as the phenotype analyses to unravel the biological role of PA3973. Transcriptional profiling of *P. aeruginosa* PAO1161 overexpressing PA3973 showed changes in the mRNA level of 648 genes. Concomitantly, ChIP-seq analysis identified more than 300 PA3973 binding sites in the *P. aeruginosa* genome. A 13 bp sequence motif was indicated as the binding site of PA3973. The PA3973 regulon encompasses the PA3972-PA3971 genes encoding a probable acyl-CoA dehydrogenase and a thioesterase. In vitro analysis showed PA3973 binding to PA3973p. Accordingly, the lack of PA3973 triggered increased expression of PA3972 and PA3971. The Δ PA3972-71 PAO1161 strain demonstrated impaired growth in the presence of stress-inducing agents hydroxylamine or hydroxyurea, thus suggesting the role of PA3972-71 in pathogen survival upon stress. Overall our results showed that TetR-type transcriptional regulator PA3973 has multiple binding sites in the *P. aeruginosa* genome and influences the expression of diverse genes, including PA3972-PA3971, encoding proteins with a proposed role in stress response.

Keywords: *Pseudomonas aeruginosa*; TetR-like transcriptional regulator; PA3973; gene expression regulation; stress response



Citation: Kotecka, K.; Kawalek, A.; Modrzejewska-Balcerek, M.; Gawor, J.; Zuchniewicz, K.; Gromadka, R.; Bartosik, A.A. Functional Characterization of TetR-like Transcriptional Regulator PA3973 from *Pseudomonas aeruginosa*. *Int. J. Mol. Sci.* **2022**, *23*, 14584. <https://doi.org/10.3390/ijms232314584>

Academic Editor: Joao Paulo Gomes

Received: 28 October 2022

Accepted: 19 November 2022

Published: 23 November 2022

Publisher's Note: MDPI stays neutral with regard to jurisdictional claims in published maps and institutional affiliations.



Copyright: © 2022 by the authors. Licensee MDPI, Basel, Switzerland. This article is an open access article distributed under the terms and conditions of the Creative Commons Attribution (CC BY) license (<https://creativecommons.org/licenses/by/4.0/>).

1. Introduction

Pseudomonas aeruginosa is a bacterium commonly found in various ecological niches and characterized by the ability to survive in very unfavorable, frequently changing environmental conditions. It is also an opportunistic human pathogen, causing infections in immunocompromised and cystic fibrosis patients, and it is often isolated from infected pulmonary and urinary tracts, eyes, or burn wounds [1]. Currently, in the pandemic era of the Coronavirus disease (COVID-19) causing severe acute respiratory syndrome, *P. aeruginosa* is one of the most frequently detected co-existent bacterial pathogen with COVID-19 among hospitalized patients with 12% confirmed detections, along with *Haemophilus influenzae* (12%) and *Mycoplasma pneumoniae* (42%) [2]. *P. aeruginosa* can increase the risk of serious complications during infection and lead to higher morbidity and mortality. It can be easily transferred, because it can survive in varying conditions, such as aquatic environments, soil, plant, and animal tissues. The success of *P. aeruginosa* as a pathogen is largely connected to its intrinsic resistance to antimicrobial agents and the broad spectrum of acquired resistance mechanisms making the treatment of *P. aeruginosa* infections a growing problem [3]. In addition to virulence and resistance factors, these bacteria modulate metabolism in response to stress factors, including antibiotics [4,5]. Thus, it is essential to understand the mechanisms responsible for the adaptation of bacteria to various environmental conditions

promoting survival and pathogenesis [6]. Gene expression control and cellular metabolism reprogramming play a pivotal role in adaptation. Elements responsible for the regulation of cellular processes, survival, and bacterial virulence during infection may be considered as potential new targets of anti-bacterial therapies [7].

P. aeruginosa is an example of a bacterium with an extensive regulatory network, in which transcriptional regulators comprise a crucial group controlling most cellular processes in response to environmental conditions [8,9]. A high number of genes encoding transcriptional regulators belonging to different families (492 genes in PAO1 reference strain) suggests their importance in *P. aeruginosa* cells [10,11]. The complexity of gene expression regulation in *P. aeruginosa* can be exemplified by the regulatory network controlling virulence or biofilm formation, which is tightly connected with the regulation of quorum sensing, antibiotic resistance, and pathogenicity [12,13].

The TetR/AcrR family of transcriptional regulators comprises an important group of regulatory factors that are well represented and widely distributed among bacteria [14]. They are involved in the control of various cellular processes, with known representatives engaged in the regulation of efflux pumps and transporters, conferring tolerance to toxic compounds and antibiotic resistance, like tetracycline repressor TetR from *Enterobacteriaceae* [15].

The TetR/AcrR-like regulators possess a two-domain structure with a DNA-binding helix-turn-helix (HTH) motif localized in the N-terminal part of the protein and a regulatory, ligand binding domain located at the C-terminus [15]. The C-terminal part contains several regions that can be involved in the binding of effectors (e.g., drugs) and in oligomerization, which can also serve as a signal to modulate the activity of the regulator. Most of the TetR-like regulators act as dimers (e.g., TetR and CamR), while others (e.g., QacR) bind a cognate operator as a pair of dimers; EthR seems to bind as an octamer [16–19]. The crystal structures of TetR family members showed conserved structures built of 9–12 helices with the DNA-binding domains formed by three helix bundles and part of the adjacent helix [18]. The second and third helices create an HTH motif, with the third called the recognition helix, as it inserts into the DNA major groove [14].

The archetype of this family of bacterial transcriptional regulators, TetR encodes a part of the most common resistance mechanism against tetracycline in Gram-negative bacteria [14]. The regulator binds as a dimer to two palindromic operator sites *tetO* repressing the expression of *tetA*, a gene encoding the tetracycline exporting protein [18]. In the presence of tetracycline, the complex of TetR with antibiotics and a magnesium ion is created, abolishing TetR binding to DNA and leading to derepression of the *tetA* and *tetR* genes [20]. The other example of regulation of the drug efflux operon by a TetR family member is the AcrR repressor involved in the regulation of drug efflux operon *acrAB* in *Escherichia coli* [15,21]. Products of this operon are part of the AcrAB-TolC tripartite transporter that effluxes substrates from the periplasm across the outer membrane out of the cell [22] and concomitantly a wide range of compounds may modulate AcrR binding to DNA [21]. Studies involving multiple TetR-type regulators indicated that these proteins may act as sensors of the environment to regulate the expression of genes in response to various stimuli [14,15]. Several of these factors are engaged in the repression of genes for cell envelope permeability and membrane transport. They regulate the expression of genes involved in antibiotic production, stress response, modulation of basic metabolism, transport systems, resistance to antibiotics, and host-encoded defense mechanisms, as well as pathogenesis [23].

The 38 representatives of the TetR family are encoded in the *P. aeruginosa* PAO1 reference genome, but only a few were characterized in detail. The best known is MexZ (PA2020), which represses the *mexXY* operon encoding the multidrug transporter, which confers resistance to various antimicrobials, including aminoglycosides [24]. The MexZ dimer binds to a 20-bp palindromic sequence in the intergenic region between *mexXY* and *mexZ* genes repressing their transcription [25,26]. The repression is alleviated in response to aminoglycosides, tetracyclines, and macrolides or oxidative stress [27–30], which does

not involve MexZ interaction with antimicrobials but depends on the action of MexZ anti-repressor ArmZ (PA5471) [26,31,32], which targets the N-terminal domain of MexZ [33].

Another characterized member of the family, CifR (PA2931), acts as a repressor of the *cif* (PA2934) gene encoding a virulence factor secreted by *P. aeruginosa* known as CFTR inhibitory factor [34,35]. Whereas most members of the TetR family act as repressors, some, including *P. aeruginosa* Pip (PA0243), were also shown to be involved in the positive regulation of gene expression, in the case of Pip, genes engaged in production of pyocyanin, another potent virulence factor [36].

The PA3973 protein from *P. aeruginosa* has been classified in silico as a putative TetR-type transcriptional regulator. Based on the PseudomonasNet, a genome-wide functional network of *P. aeruginosa* genes, a negative regulation of transcription, DNA-dependent, and cellular response to stress are predicted for PA3973 according to GO terms [37]. The PA3973 gene was previously identified as significantly upregulated in cells lacking *vqsM*, a crucial component of quorum sensing [38], but also in *P. aeruginosa* *parA* and *parB* mutants, which showed disturbed chromosome segregation [8,39]. This study aimed to decipher the function of this regulator.

2. Results

2.1. Overview of the PA3973 from *P. aeruginosa*

PA3973 is the first gene of the PA3973-PA3970 gene cluster in the *P. aeruginosa* PAO1 genome, encoding a protein classified as a TetR-type putative transcriptional regulator (Figure 1A). The structure prediction showed two potential domains in PA3973 with the N-terminally located HTH motif encompassing amino acids 14–74 (helices α_2 and α_3) possibly involved in contact with DNA [40] and the C-terminal part, creating a putative ligand-binding domain responsible for signal perception and dimerization (Figure 1B). Two monomers of PA3973 possibly form a dimer (Figure 1C), similarly to other members of the TetR family [14,15]. The ability of the protein to self-assemble was confirmed using glutaraldehyde crosslinking of purified His₆-PA3973 followed by a Western blot analysis (Figure 1D). The assay showed additional bands migrating just above the target dimer, which likely reflects various conformational states of the crosslinked dimer.

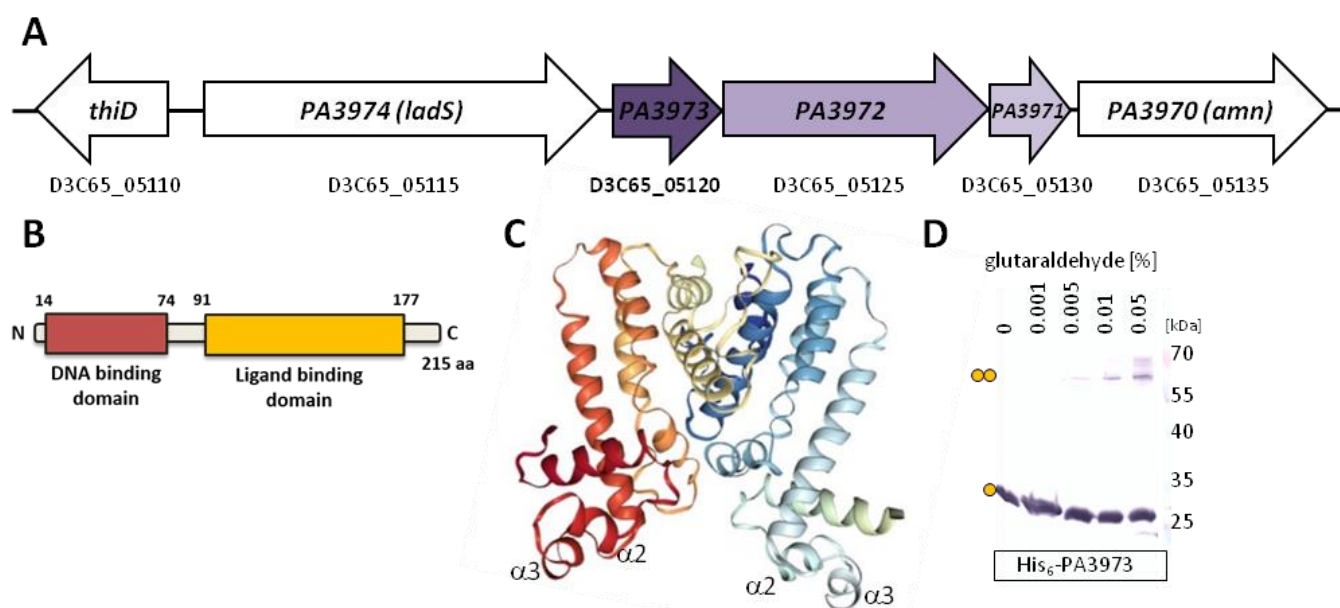


Figure 1. Properties of PA3973 protein from *P. aeruginosa*. (A) Genomic context of the PA3973 gene in the *P. aeruginosa* PAO1 genome. The gene names from PAO1161 and PAO1 strains are presented below and inside the arrows representing loci, respectively. The PA3973-PA3972-PA3971 gene cluster is shown in shades of purple. (B) Domain structure of PA3973 protein. (C) Structural model of PA3973

dimer obtained using AlphaFold2 and HDOCK [40,41]. Monomers are coloured in shades of red to khaki or navy blue to olive. The helices $\alpha 2$ and $\alpha 3$ constituting the HTH DNA binding domain are marked. (D) Analysis of the oligomerization state of purified His₆-PA3973 by cross-linking with glutaraldehyde. Samples were separated by SDS-PAGE (12% gel) and analyzed by Western blot using anti-His₆ antibodies. Dimeric forms are marked by two dots.

In silico analyses and database mining suggested that products of the genes encoded within the PA3973-PA3970 gene cluster could be involved in a stress response (Figure 1A). They encode a probable acyl-CoA dehydrogenase, *E. coli* AidB homolog (PA3972), a putative thioesterase from PaaI family (PA3971), and an AMP nucleosidase, Amn (PA3970). According to the Pseudomonas Database, the PA3973-PA3970 genes are predicted to form an operon, but since experimental evidences are lacking, throughout this manuscript, the term gene cluster is used.

2.2. Identification of PA3973-Regulated Genes and Binding Sites for This Transcriptional Regulator in the *P. aeruginosa* Genome

To analyze the role of PA3973 in *P. aeruginosa*, a PAO1161 Δ PA3973 mutant was constructed. This mutant strain did not display obvious differences in growth in LB or M9 medium, swimming, swarming, twitching, or biofilm formation compared to the wild type (WT) parental strain PAO1161 (Figure 2A,B). In parallel, the effect of PA3973 overexpression was tested by linking the gene to an IPTG (isopropyl- β -D-thiogalactopyranoside)-inducible promoter in plasmid pKKB3.11 (*lacI^q-tacp-PA3973*). No effect of PA3973 overproduction on bacterial growth was observed in *P. aeruginosa* under the tested gradient of IPTG in the growth medium (Figure 2C).

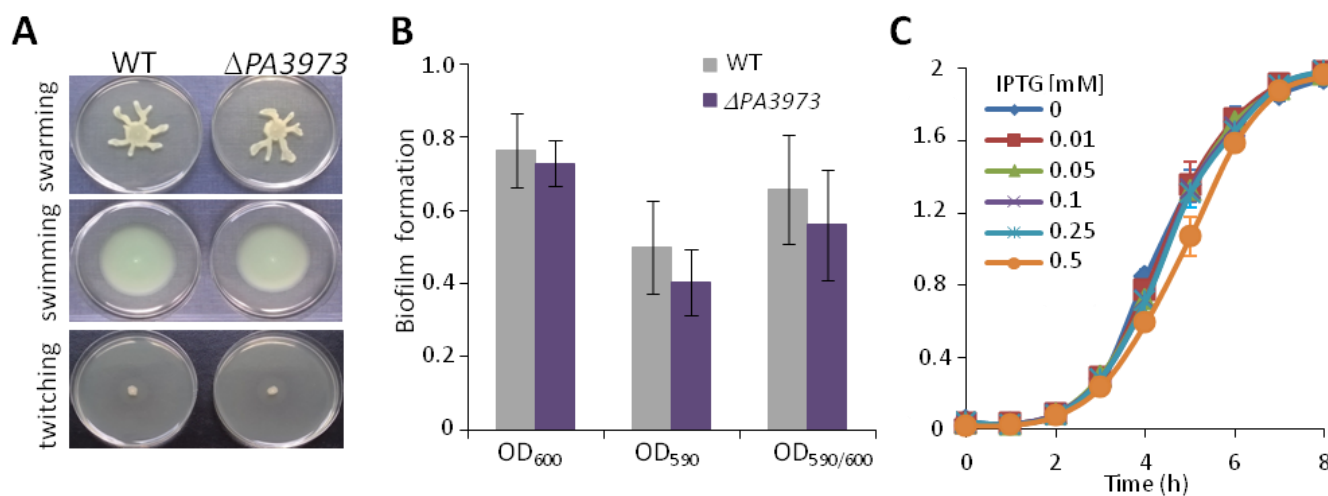


Figure 2. Phenotype analysis of *P. aeruginosa* PAO1161 WT, Δ PA3973, and PA3973 overproducer strains. (A) Selected pictures of swimming, swarming, and twitching analyses of WT *P. aeruginosa* PAO1161 and Δ PA3973 mutant. (B) Biofilm formation of WT *P. aeruginosa* PAO1161 and Δ PA3973 mutant. Cultures were grown without shaking in LB medium at 37 °C for 24 h and biofilm content measurements were performed. Data represent mean \pm SD from 6 biological replicates. No statistically significant changes were observed by comparing Δ PA3973 with WT ($p > 0.05$ in a two-sided Student *t* test). (C) Growth curves of *P. aeruginosa* PAO1161 cells carrying pKKB3.11 (*tacp-PA3973*) grown under selection in LB in the presence of different concentrations of IPTG. Data represent mean \pm SD from 3 biological replicates.

To identify genes that display PA3973-dependent expression, we used RNA sequencing analysis (RNA-seq). In addition, we performed chromatin immunoprecipitation and sequencing analysis (ChIP-seq) to identify PA3973 binding sites in the *P. aeruginosa* genome. The rationale behind an analysis of cells with PA3973 in excess was based on the following: (i) the relatively low level of PA3973 expression under standard growth conditions (LB or

M9 medium; Bartosik AA, personal communication); (ii) the likelihood that an excess of PA3973 might mimic the induced, activated state of the protein; and (iii) the fact that the effector, signal, or partner for this TetR-type regulator is unknown.

RNA-seq was performed using material isolated from cultures of the strains PAO1161 pKKB3.11 (*tacp-PA3973*, hereafter called PA3973+) and PAO1161 pAMB9.37 (*tacp*, empty vector [EV]) grown in a selective LB medium supplemented with 0.05 mM IPTG (Figure 2C; Table S3). The comparison of the PA3973+ and EV transcriptomes showed 648 loci with altered expression (fold change [FC] ≤ -2 or ≥ 2 , adjusted *p*-value ≤ 0.01) (Figure 3A; Table S3). The expression of 374 loci was downregulated, whereas 274 loci displayed increased expression. For convenience, we use the *P. aeruginosa* PAO1 gene names throughout the manuscript, although the corresponding PAO1161 gene names are also included. The functional classification of the identified loci, based on PseudoCAP [11], showed that the upregulated genes were mostly associated with protein secretion/export systems, non-coding RNA, and cell wall functions (Figure 3B; Table S3). Decreased expression was observed for several genes encoding proteins engaged in energy metabolism, chemotaxis, central intermediary metabolism, or adaptation and protection. The most significantly downregulated genes were *norC* from the PA0509-PA0527 gene cluster, *nosR* from the PA3391-PA3393 cluster, *narK1* from the PA3874-PA3880 gene cluster, *ccoP2* from the PA1555-PA1557 cluster, *arcD* from the PA5170-PA5173 operon, or *nrpD* from the PA1919-PA1920 gene cluster. Concomitantly, the most significantly upregulated loci were PA5024, PA4193 from the PA4191-PA4195 cluster, *cysT* from the PA0280-PA0284 cluster, PA3445-PA3446, PA2311, and PA3530 (Figure 3B; Table S3).

The RT-qPCR (reverse transcription followed by quantitative PCR) analysis was performed to validate the changes in gene expression in the PA3973 overproducer strain in an independent set of biological replicates, collected at the same conditions as used for the RNA-seq analysis (Figure 3C). The genes selected for the RT-qPCR analysis had a broad range of fold changes observed in PA3973+ vs. EV cells, and the selected reference gene *proC* (PA0393) was not altered in the tested conditions based on RNA-seq results. Essentially, most of the RT-qPCR results correlated well with the RNA-seq data, confirming a negative impact of PA3973 on the expression of PA3614, PA5208, PA5460, PA5497, and PA3972 (Figure 3C).

To identify PA3973 binding sites in the *P. aeruginosa* genome, ChIP-seq analysis was performed using anti-FLAG antibodies and Δ PA3973 cells carrying plasmid pMEB255 (*tacp-PA3973-flag*), which were grown in a selective LB medium supplemented with 0.05 mM IPTG. As a background control for the ChIP procedure, the Δ PA3973 strain carrying plasmid pABB28.1 (*tacp-flag*) was grown under the same conditions, and samples were processed in parallel. The comparison of PA3973-FLAG ChIP samples with control samples using a fold enrichment (FE) cut-off value of 2 (Figure 4A) yielded 308 PA3973-FLAG ChIP-seq peaks. The summits of 139 peaks (45%) mapped to intergenic regions (Table S4), suggesting the potential of PA3973 to regulate the expression of adjacent loci. The summits of 169 peaks mapped to gene bodies (coding regions) (Table S5). A search for nucleotide motifs shared by sites bound by PA3973 using MEME [42] showed the presence of a 13 bp motif SAAGRNMGTGAACG, where S-G or C; R-A or G; M-A or C (Figure 4B) based on the analysis of 100 bp regions encompassing summits of all 308 peaks indicating PA3973 binding sites.

The functional PseudoCAP analysis of genes potentially influenced by PA3973, based on the ChIP-seq results, demonstrated enrichment in genes encoding proteins engaged in secretion/export systems, adaptation and protection, and central intermediary metabolism (Figure 4C). Table A1 (Appendix A) lists the most enriched PA3973 bound sites (FE > 4) under the tested conditions and adjacent genes, in which expression could be modulated. This data indicates that PA3973 has multiple binding sites in the *P. aeruginosa* genome, which suggests that this factor may function as a crucial component of the gene expression regulatory network.

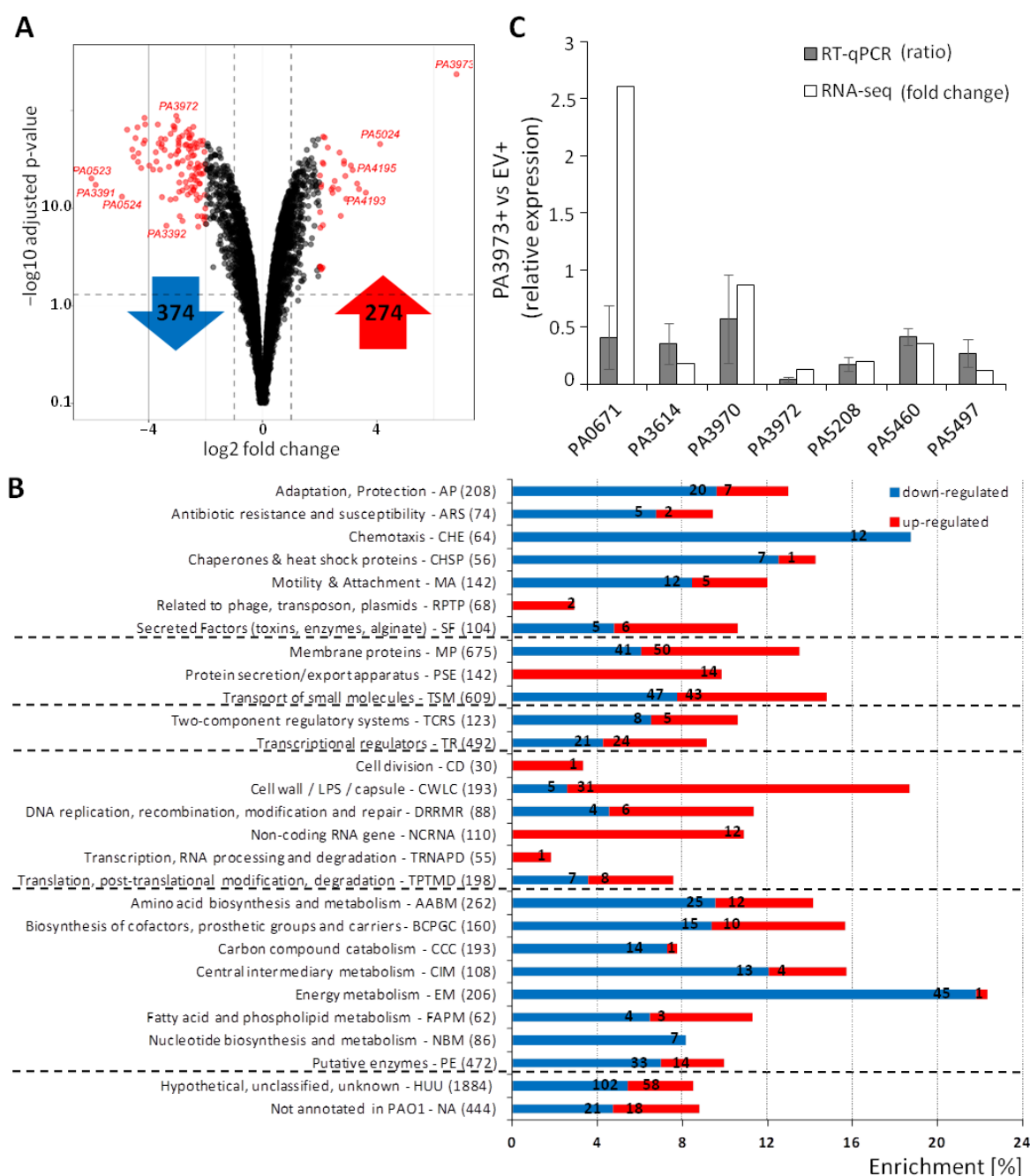


Figure 3. Identification of PA3973 dependent genes in *P. aeruginosa* using RNA-seq. Transcriptomes of PAO1161 cells carrying pKKB3.11 (*tacp-PA3973*) or pAMB9.37 (*tacp*), grown under selection in LB supplemented with 0.05 mM IPTG were analyzed by RNA-sequencing. **(A)** Volcano plot of RNA-seq data comparing the transcriptomes of PA3973+ and EV cells. Most significantly altered genes are indicated in red. The numbers of up- and down-regulated loci are presented in red and blue arrows, respectively. **(B)** Classification of loci (as in Table S3) with altered expression in response to PA3973 excess according to PseudoCAP categories [11]. The bars indicate the enrichment of genes belonging to each category relative to all genes from the category in the PAO1 genome. Numbers presented in red and blue bars correspond to the numbers of up- and down-regulated genes, respectively, in each category. **(C)** Validation of RNA-seq data by RT-qPCR analysis. The RT-qPCR was performed using RNA samples obtained for the same conditions of growth as samples used for RNA-seq analysis. The results of RNA-seq data are presented as a fold change according to data presented in Table S3, while RT-qPCR data represent the mean ratio \pm SD for three biological replicates of PA3973+ cells relative to mean expression of the control EV+ strain.

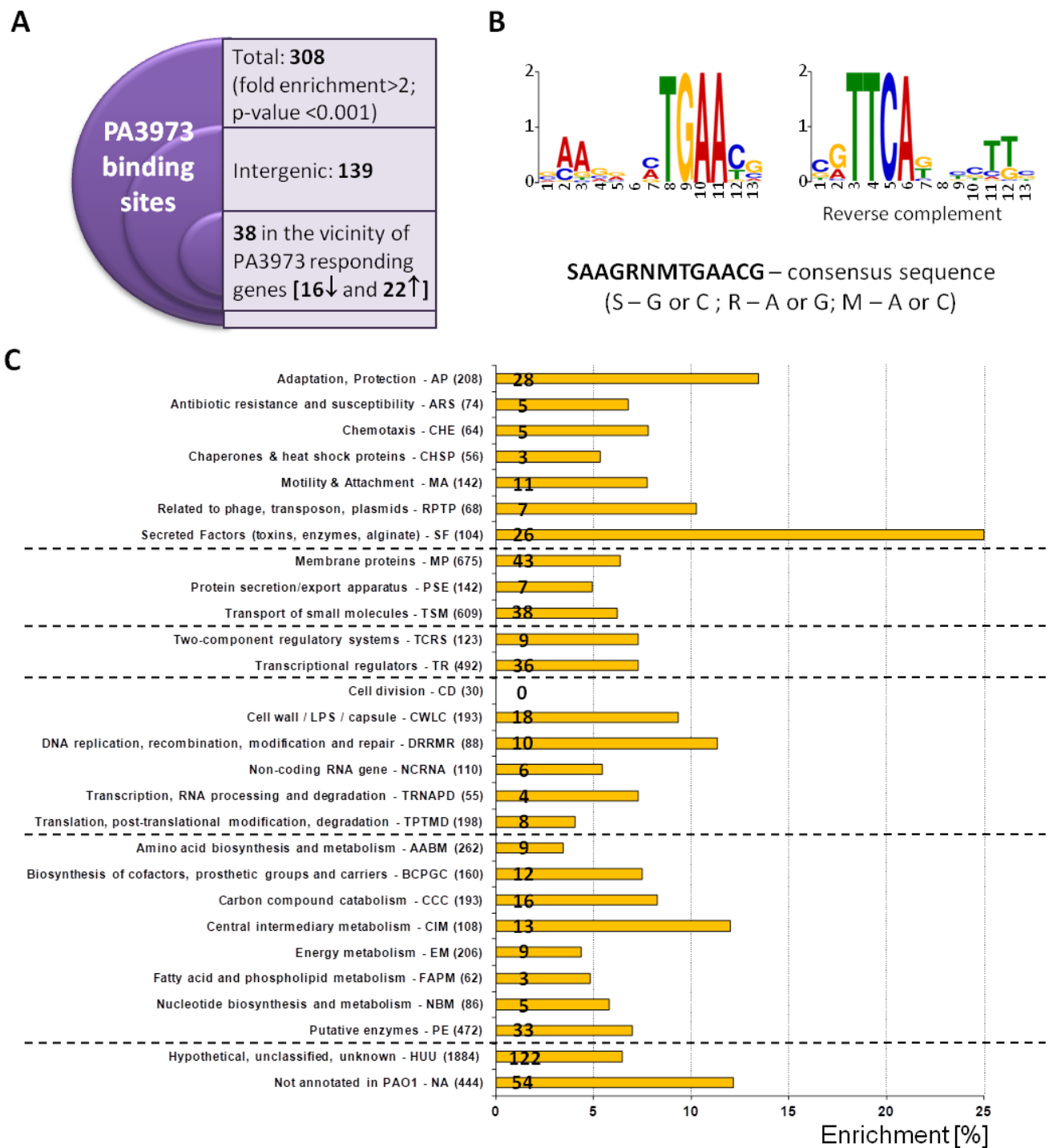


Figure 4. Identification of PA3973 binding sites in *P. aeruginosa* (ChIP-seq). (A) Cells expressing PA3973-FLAG were subjected to chromatin immunoprecipitation using anti-FLAG antibodies. Reads obtained by sequencing the ChIP DNA were mapped onto the PAO1161 genome. A gene was classified as likely to be directly regulated by PA3973 if the ChIP-seq peak summit was located in the vicinity of the start codon of the gene affected in RNA-seq by PA3973 excess. (B) Sequence logo of the PA3973 binding motif and its reverse complement version obtained by MEME tool [42]. The proposed consensus sequence is presented below. (C) Functional classification of genes likely to be affected by PA3973 binding. Bars present the enrichment of loci with PA3973 binding sites identified in ChIP-seq in the vicinity of genes and coding regions (identified genes from Tables S4 and S5), belonging to each PseudoCAP category [11]. Numbers indicate the exact number of genes belonging to each category with PA3973 binding site in their vicinity.

2.3. Genes under the Direct Control of PA3973

Importantly, 38 of the 648 genes showing altered expression in response to a PA3973 excess possessing a binding site for this transcriptional regulator within their promoter regions or adjacent to these genes (Figure 4A and Table A2). In addition, 26 detected in coding regions were located in the vicinity of genes that showed changes in expression level in RNA-seq analysis (Table S5), but the mechanism by which PA3973 could influence their expression requires further studies.

The ChIP-seq analysis indicated that PA3973 binds within the region preceding its own coding sequence, in agreement with its effect on the expression of the downstream located PA3972-PA3971 genes (Table A1). The PA3973 binding site with the second highest fold enrichment, besides the PA3973 promoter region, was detected in the putative promoter of PA4156, encoding a protein highly homologous to the *Vibrio cholerae* vibriobactin receptor (ViuA) involved in iron acquisition [43]; however, no significant changes in PA4156 expression were detected under tested conditions in our RNA-seq analyses (Table A1).

A PA3973 binding site was also detected in the putative promoter of PA1673, the gene showing the most severe downregulation in the RNA-seq analysis (Table A2), as well as in promoter regions of PA3762 and PA3531 that were downregulated in response to PA3973 excess (Table A2). Interestingly, the PA3530, which was transcribed up-stream from the PA3531 gene, also showed changes in expression under PA3973 overproduction but with significantly increased mRNA level (Table A2).

Similarly, the PA2468, encoding a sigma factor FoxI [44], had a peak in the region preceding the gene (Table A2). Interestingly, three other genes coding for RNA polymerase sigma factors PA2426, PA3899, and PA0715 exhibited changes in expression in response to PA3973 and possess PA3973 binding sites in their promoter regions (Table A2).

To confirm the interactions of PA3973 with the selected regions, we performed electrophoretic mobility shift assays (EMSA) using purified PA3973-His₆ and DNA fragments corresponding to the putative promoter regions of the genes exhibiting the highest fold enrichment in ChIP-seq analysis: PA3973, PA4156, PA4710, PA0061, PA2722, PA0195, and PA2468 (Table A1). PA3973-His₆ was able to specifically bind to PA3973p in a concentration-dependent manner (Figure 5A). The EMSA assay also showed PA3973-His₆ interactions with putative promoters of PA0061, PA0195, and PA2722 (Figure 5C,D,F). No clear shifted DNA-protein complexes, but a disappearance of unbound specific DNA in the presence of the higher concentration of the protein, could be observed in the case of the PA2468p, PA4156p, or PA4710p (Figure 5E,G,H) in tested conditions. It is possible that additional factors (e.g., a cellular partner, and/or the presence of the ligand) might be required for the efficient PA3973 binding to these sites.

All tested promoters contained sequences matching the motif SAAGRNMGTGAACG predicted using MEME (Figures 4B and 5I). In the case of PA3973p, this motif appeared twice and is a part of palindromic and pseudopalindromic sequences (TGAATCC GGATTCA and TGAAGCG TGATTCA, respectively) encompassing the predicted -10 sequence of PA3973p (Figure 5I). To verify the importance of the identified palindromic sequence in DNA binding by PA3973, a variant of the PA3973 promoter fragment (PA3973p*) lacking the fragment encompassing the TGAATCCGGATTCA palindrome and a part of the pseudopalindrome was tested in an EMSA. PA3973-His₆ was not able to bind to this variant of PA3973p, suggesting the involvement of these sequences in the protein recruitment to this promoter (Figure 5B,I).

To further examine the influence of PA3973 on the expression of the aforementioned genes, their promoter regions were cloned upstream of a promoter-less *xylE* gene in the vector pPTOI. Out of the selected genes, only PA2468 and PA4156 promoters were active in the heterologous host *E. coli* DH5 α (Figure 5J). The expression of PA3973 in cells carrying a plasmid with PA4156p-*xylE* resulted in significantly reduced XylE activity in the corresponding cell extracts, but no such regulation was observed for PA2468p-*xylE* under the tested conditions (Figure 5J).

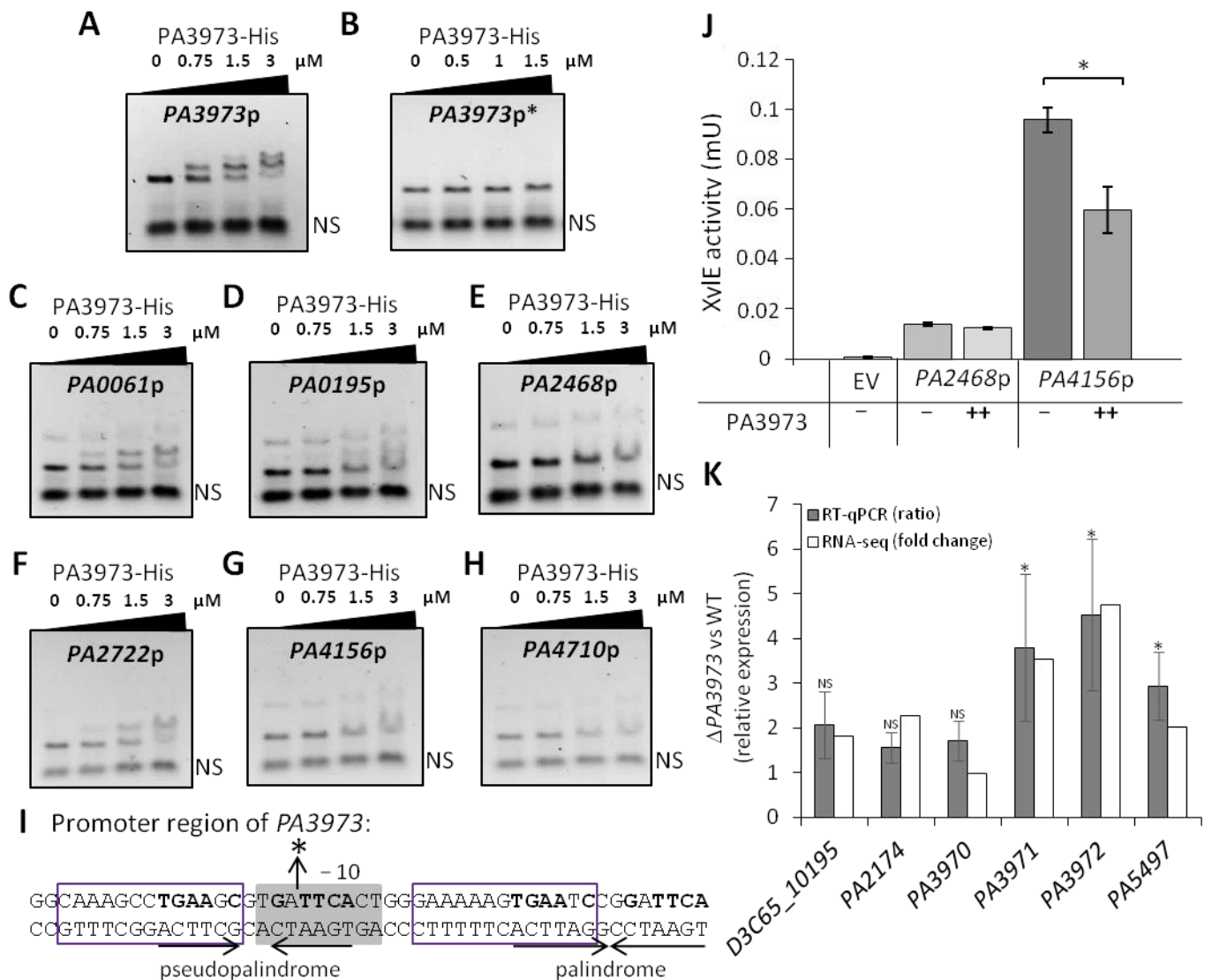


Figure 5. Regulatory properties of PA3973 assayed in vitro and in vivo. EMSA analysis of PA3973-His₆ binding to regions preceding PA3973 [long (A) and short promoter fragment (B)], PA0061 (C), PA0195 (D), PA2468 (E), PA2722 (F), PA4156 (G), PA4710 (H). Amplified DNA fragments were incubated with the indicated amounts of the protein in the presence of unspecific, competitor DNA (marked as NS), and complexes were separated by electrophoresis on 1.5% agarose gel. Ethidium bromide staining was used for the visualization of DNA. (I) Sequence preceding the PA3973 gene. Probable binding motifs are marked with the purple box. "*" indicates the site of truncation of PA3973p to obtain its shorter fragment. (J) XylE activity in *E. coli* DH5α carrying pMEB267 (PA2468p-*xylE*) or pMEB269 (PA4156p-*xylE*) with pKKB3.11 (*tacp*-PA3973) (++) or empty plasmid pAMB9.37 (-). Strains were grown in selective LB with supplementation of 0.2 mM IPTG for pKKB3.11 (++) Cells carrying the promoter-less pPTOI (-*xylE*) (EV) and pAMB9.37 were used as background control. The data represent the means ± SD and * indicates $p < 0.05$ in a Student's two-tailed *t*-test. (K) The genes with altered expression in ΔPA3973 strain vs. WT PAO1161 as indicated by RNA-seq analysis and RT-qPCR analysis carried out using RNA samples obtained for the same conditions as samples used for RNA-seq analysis. The results of RNA-seq data are presented as a fold change according to data presented in Table S6, while RT-qPCR data are presented as a ratio. Data represent mean ratio ± SD for three biological replicates. * indicate significantly different expression (ratio > 2, p -value < 0.05 in two-sided Student's *t*-test assuming equal variance) comparing ΔPA3973 with WT using the *proC* reference gene; NS—not significant.

To further define the targets of PA3973 action, we performed an RNA-seq analysis of PA3973-deficient cells relative to WT cells, which showed significantly increased PA3972 and PA3971 transcript levels, confirming the role of PA3973 in PA3972-PA3971 repression (Figure 5K; Table S6). Additionally, three genes, PA2174, PA5497, and D3C65_10195, also exhibited increased mRNA levels in the absence of PA3973, indicating a possible involvement of this regulator in their control. The RT-qPCR verification of the changes observed in the RNA-seq analysis showed the direction of changes to be consistent for both analyses, confirming the influence of PA3973 on the expression of these genes (Figure 5K). Overall, this data confirmed that PA3973 binds to DNA fragments identified in the ChIP-seq analysis and may regulate the activity of target promoters to influence gene expression.

2.4. Towards the Biological Function of PA3973-PA3971 Gene Cluster

In silico analyses and database mining suggested that the products of the PA3973-PA3971 gene cluster could potentially be involved in stress response. Besides the first gene coding for the TetR-type transcriptional regulator PA3973, this cluster also encodes a probable acyl-CoA dehydrogenase (PA3972) and a putative thioesterase (PA3971). The PA3972 from *P. aeruginosa* is the putative homolog of the AidB protein from *E. coli* (41% identity, 56% similarity) with possible acyl-CoA dehydrogenase activity and oxidoreductase activity, acting on the CH-CH group of donors [11]. The AidB protein is involved in the defense against methylating agents [45–47]. In *E. coli*, *aidB* was upregulated in response to small doses of DNA-methylating agents [48]. This gene, along with *alkA* and *alkB*, belongs to the Ada protein regulon that controls the cellular stress response induced by the presence of alkylating agents, leading to changes in DNA or RNA [49].

The PA3971 gene encodes a hypothetical protein belonging to the thioesterases family [11]. Its expression level increases when the strain is subjected to stress factors such as hydrogen peroxide [50]. A BLAST analysis showed approximately 40% similarity to a thioesterase from *E. coli*, which is responsible for the degradation of phenylacetic acid [51], and a high 91% similarity to a putative esterase from *Acinetobacter baumannii* with a role in the biosynthesis of secondary metabolites.

To assign a biological function to PA3972 or PA3971, the chromosomal double mutant of PAO1161 in PA3972-71 genes was constructed. No changes in colony morphology, bacterial motility, or biofilm formation were observed between the Δ PA3972-71 mutant and the WT strain. Lack of PA3973 or PA3972-71 did not significantly affect the growth of the cells in a rich medium, or minimal M9 or MOPS medium supplemented with glucose as the carbon source in the early stages of culture growth (Figure 6A,D,G). However, prolonged incubation over eight hours (and up to 48 h in the case of a MOPS medium) resulted in a significantly lower OD₆₀₀ of the Δ PA3972-71 mutant and to a less extent for Δ PA3973 in comparison with the WT strain (Figure 6G). This suggests that in conditions that might involve stress possibly connected with starvation, the PA3973, PA3972, and/or PA3971 proteins might play an important role in facilitating pathogen survival. The growth in the presence of hydroxylamine and hydroxyurea, two stress-inducing agents, was also tested (Figure 6B,C,E,F). Hydroxylamine exposure introduces mutations by acting as a DNA nucleobase amine-hydroxylating agent [52], whereas hydroxyurea is a ribonucleotide reductase inhibitor, altering DNA replication and nucleotide metabolism by the depletion of deoxyribonucleoside triphosphate pool [53].

The presence of hydroxylamine (50 μ g/mL) or hydroxyurea (1–20 mM) tested in an LB and M9 minimal medium with glucose slowed down the growth of *P. aeruginosa* strains in comparison to growth in a medium without these compounds (Figure 6A–F). The presence of hydroxylamine caused a prolonged lag time of bacterial culture growth with a significantly slower kinetic of the Δ PA3972-71 strain in comparison with the WT or Δ PA3973 in M9 medium (Figure 6E), indicating that PA3972 and/or PA3971 could facilitate the growth of bacteria in such conditions.

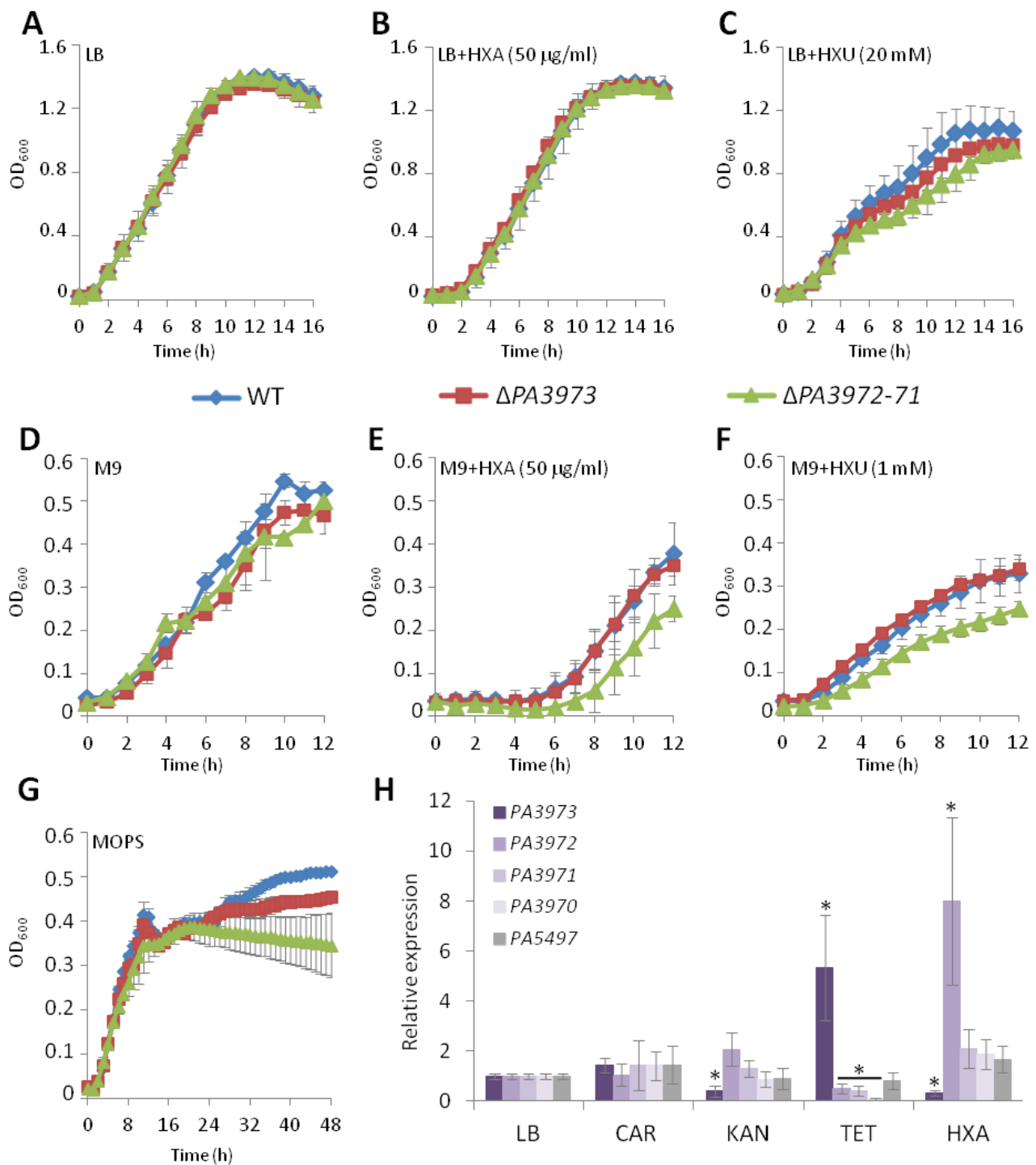


Figure 6. Involvement of *PA3973-PA3971* gene cluster in response of *P. aeruginosa* to stress. Kinetics of growth of *P. aeruginosa* strains PAO1161 WT, $\Delta PA3973$ and $\Delta PA3972-71$ at 37 °C in indicated media in the presence of hydroxylamine and hydroxyurea: LB (A), LB + 50 $\mu\text{g/ml}$ hydroxylamine (B), LB + 20 mM hydroxyurea (C), M9 + glucose (D), M9 + glucose + 50 $\mu\text{g/ml}$ hydroxylamine (E), M9 + glucose + 1 mM hydroxyurea (F), MOPS + glucose (G). Data represent mean \pm SD from three independent experiments. HXA-hydroxylamine; HXU-hydroxyurea. (H) Relative expression of indicated genes in WT PAO1161 cells cultured in LB medium without antibiotic [LB] and with different classes of antibiotic added at subinhibitory concentrations: carbenicillin, 32 $\mu\text{g/ml}$ [CAR]; kanamycin, 10 $\mu\text{g/ml}$ [KAN], and tetracycline, 4 $\mu\text{g/ml}$ [TET]. Additionally, the expression of indicated genes in cells grown with hydroxylamine (50 $\mu\text{g/ml}$) [HXA] added to the medium was tested and compared to the control [LB]. * $p < 0.05$ in a Student two-sided t -test assuming equal variance.

The significantly slower growth of $\Delta PA3972-71$ cultures in comparison with the WT, was also observed in the presence of 20 mM (in LB medium) or 1 mM (in M9 medium) hydroxyurea (Figure 6C,F). This data indicates that PA3972 and/or PA3971 may play a role in stress response; however, further studies are needed to discover the underlying mechanisms.

The RT-qPCR analysis was also applied to check the expression of PA3973 and selected genes from its regulon in the *P. aeruginosa* WT cells exposed to antibiotics and hydroxylamine. The analysis showed no significant difference in the PA3973 expression upon the addition of carbenicillin compared to control cultures (non-treated grown in LB), but significantly decreased the expression in response to kanamycin, and increased the mRNA level of PA3973 in response to tetracycline (Figure 6H). Interestingly, the expression of PA3972-PA3970 genes was significantly downregulated in response to tetracycline (Figure 6H), which correlates with the increased expression of PA3973, confirming its repressor functions for the PA3972-71 genes. Moreover, in the presence of hydroxylamine, the expression of PA3973 was significantly down-regulated, and the PA3972, but not PA3971 or PA3970, showed a notable up-regulation, which suggests that PA3972 expression is induced in response to hydroxylamine.

This data indicates that PA3973 action might be connected with the cellular response to some stressors, but further studies are needed to discover the underlying mechanisms and the role of PA3973-dependent genes, including PA3972, in this process.

3. Discussion

The PA3973 of *P. aeruginosa* based on sequence similarity is classified as the TetR-type transcriptional regulator. The N-terminal part, similar to other members of the TetR family, consists of the HTH DNA-binding domain predicted with structure modeling, in which helices $\alpha 2$ and $\alpha 3$ are involved in direct contact with cognate DNA [14,15]. The C-terminal part is presumably involved in signal perception and oligomerization. The presence of a dimeric form was confirmed with glutaraldehyde cross-linking experiments with the use of purified His₆-PA3973. The signal to which PA3973 responds in *P. aeruginosa* awaits elucidation.

The ChIP-seq was applied to evaluate the binding of PA3973 across the chromosome in exponentially growing *P. aeruginosa* cells. The 308 PA3973-binding targets located across the genome, including intergenic and coding regions, were identified. Multiple binding sites in the genome suggest the role of PA3973 as a global regulator of gene expression in *P. aeruginosa*. However, the transcriptional profiling of $\Delta PA3973$ mutant cells grown in rich medium did not support the global impact. Significantly, under this conditions, the increased expression of PA3972, PA3971, PA2174, and PA5497 genes was detected in PA3973 deficient cells in comparison with the WT (Figure 5K; Table S6). In contrast, the RNA-seq analyses of exponentially growing cells overproducing PA3973 showed 648 genes responding to PA3973 (Table S3). Among them 38 genes possess PA3973 binding sites in their promoter regions or in the vicinity of these genes and the additional 26 genes in coding regions (Table A2, Tables S4 and S5). These genes could exhibit direct PA3973-dependent regulation in contrast to the remaining loci with altered expression in PA3973 overexpressing cells, which likely represent the indirect effect of PA3973 action on *P. aeruginosa* cells.

In the case of most transcriptional regulators their high-affinity binding sites are largely restricted to non-coding DNA regions to exert direct effect on the target genes' expression [54]. In the case of PA3973, more than half (169 out of 308) of the DNA targets for PA3973 are located within the coding regions of the genome and appear to have little or no effect on gene expression, at least under the conditions tested. This may suggest that additional factors (e.g., special growth conditions, presence of ligand, signal and/or cellular partner) might be involved in PA3973 regulatory activity. A similar pattern was observed; for example, in *E. coli*, RutR, the uracil-responsive transcription factor from the TetR family involved in the regulation of the expression of the *rut* operon encoding genes

for the catabolism of pyrimidine. RutR showed multiple additional binding sites within genes; however, their role in gene expression control remains elusive [55]. Concomitantly, an interesting mode of action among TetR-like regulators exemplifies a LuxR protein from *Vibrio alginolyticus* [56]. It controls the expression of approximately 280 genes that contain either a symmetric palindrome or asymmetric binding motifs upstream, overlapping start codon, or inside open reading frames. Differences in LuxR binding to these motifs, modulated by its N-terminal extension, allow the repression or activation of cognate gene expression to impact quorum sensing and virulence [56]. Based on ChIP-seq data and the localization of identified PA3973 binding sites, we speculate that this regulator might present a similar mode of action.

The sequence analysis of PA3973 ChIP-seq peaks revealed a 13-bp binding motif with the consensus SAAGRNMGTGAACG. In the case of PA3973p, this motif was found twice in the sequence encompassing the predicted -10 promoter sequence (Figure 5I). Two closely located motifs, separated by a dozen or more base pairs, are also present in other loci identified as PA3973 targets (e.g., PA0061p, PA0195p, PA2468p, and PA4710p). One PA3973-binding motif was identified in PA2722p, PA4056p, or PA4156p. In some target regions, the binding sites for other regulatory factors could be detected, such as the Fur (ferric uptake regulation protein) binding site in PA4156p or PA4710p. This suggests that, besides PA3973, other factors might be involved in the regulation of these genes. The Fur is involved in the regulation of iron metabolism in *P. aeruginosa* (e.g., in the control of the production of receptors and siderophores involved in iron scavenging) [57]. Moreover, the PA3973 binding site was identified in the promoter region of the PA2468 encoding extracytoplasmic function sigma factor (ECF) FoxI [44].

Other interesting regulatory connections are the decreased expression of PA1920 in response to PA3973 excess (Table A1 and Table S3) and the up-regulation of PA5497 in Δ PA3973 mutant (Figure 5K; Table S6). The PA1920 and PA5497 encode a class III (anaerobic) ribonucleoside-triphosphate reductase subunit, NrdD, and a class II (cobalamin-dependent) ribonucleotide-diphosphate reductase subunit, NrdJa, respectively. Importantly, it was shown that both ribonucleotide reductases (RNR) are highly expressed during infection [58]. In *P. aeruginosa*, three different types of RNR are encoded, allowing adaptation to different environmental conditions including anaerobiosis [59,60]. The expression of RNR genes is under the control of NrdR, a global regulator, which, in *E. coli*, binds to the NrdR boxes (acaCwAtATaTaTwGtg) in the promoters of target genes [60]. Such sequences could be found in PA1920 and PA5497 promoter sequences, and the ChIP-seq data showed the PA3973 binding site in the coding sequence of PA1920 and PA5497. Moreover, the PA3973 binding site with fold enrichment 10 (Table A1) was detected in the predicted PA4056-PA4057 (*nrdR-ribD*) operon, overlapping the end of the *nrdR* and the beginning of the *ribD* ORFs. It suggests the existence of complex regulatory interdependencies, managing the expression of these genes.

The EMSA assays for the selected targets of PA3973 showed varying affinity of PA3973 to analyzed targets, with the strongest binding observed in the case of PA3973p comprising two pseudopalindromic/palindromic sequences, which likely served as the operator sequences recognized by PA3973 (Figure 5A–H). In the promoter region of PA3973, the identified PA3973 binding sites are part of two closely spaced pseudopalindromic/palindromic sequences of 14 bp in length separated by 11 bp (Figure 5I). Their arrangement and localization resemble the operator sequences of other TetR-type regulators (e.g., TetR with two 15 bp operator sequences (TCTATCATTGATAGG) separated by 11 bp) [14,18]. The deletion of the palindromic sequence and part of the pseudopalindromic sequence prevented PA3973 binding to truncated PA3973p*, suggesting that the presence of these sequences is needed for protein binding to cognate sequence and to exert a possible effect on expression (e.g., repression). It is tempting to propose the model in which PA3973 acting as a dimer binds to these operator sequences, repressing expression from its own promoter and possibly PA3972-PA3971 genes.

Our studies on *P. aeruginosa* growth in the presence of stress-inducing agents like hydroxylamine or hydroxyurea showed that PA3972 could facilitate bacterial growth in such detrimental conditions. Interestingly, it was recently shown that PA3972 belongs to negative regulators of bacterial virulence as predicted with PseudomonasNet and further validated by the analysis of the PA3972 knockout mutant in the *Caenorhabditis elegans* infection model [37]. The disruption of PA3972 resulted in elevated *P. aeruginosa* PAO1 virulence in *C. elegans*.

Taken together, these results demonstrated the participation of TetR-type transcriptional regulator PA3973 in several diverse cellular processes including the modulation of cellular response to growth conditions to keep cellular homeostasis and facilitate pathogen survival. Some of the identified PA3973 targets play a role in *P. aeruginosa* stress response and pathogenesis, but the exact mechanism and the signals to which PA3973 responds and regulates its targets need further investigation. Presented data brings us closer to understanding the complex *P. aeruginosa* system, to draw the picture of regulatory connections involved in controlling bacteria lifestyle as a free-living organism and during infection.

4. Materials and Methods

4.1. Bacterial Strains, Plasmids, and Growth Experiments

The bacterial strains used and constructed in this study (listed in Table S1) were grown in an L broth (LB) rich medium or on LB-agar at 37 °C, or in M9 or MOPS minimal medium [61] supplemented with glucose (0.5%) as the carbon source, and with leucine (10 mM) added in the case of *P. aeruginosa* PAO1161 *leu*[−] strains cultured in minimal media. Hydroxyurea (1 or 20 mM) and hydroxylamine (50 µg/mL) were used in growth experiments as indicated. For the selection of plasmids in *E. coli*, the media were supplemented with 10 µg/mL chloramphenicol, 50 µg/mL kanamycin, or benzyl penicillin at a final concentration of 150 µg/mL in a liquid medium or 300 µg/mL in agar plates. For *P. aeruginosa* strains, carbenicillin (300 µg/mL), rifampicin (300 µg/mL), and chloramphenicol (75 µg/mL in a liquid medium; 150 µg/mL in plates) were used as required. For growth experiments, cultures were grown overnight with shaking at 37 °C and diluted with fresh medium either in flasks, closed with cotton plugs, or in 96-well plates. Bacterial growth was monitored by measurements of optical density at 600 nm (OD₆₀₀) in a spectrophotometer Shimadzu UV-1800 (Shimadzu Corporation, Kyoto, Japan) or with the use of Varioskan Lux Multimode Microplate Reader and SkanIt RE software (Thermo Fisher Scientific, Waltham, MA, USA). Competent *E. coli* cells were prepared with a treatment of CaCl₂ [62]. The competent *P. aeruginosa* cells were prepared with a treatment of MgCl₂ as described previously [63].

All plasmids used and constructed in this study are described in Table S1. All primers used are listed in Table S2.

The *P. aeruginosa* PAO1161 Δ PA3973 and Δ PA3972-71 mutants were obtained with allelic exchange. The competent cells of *E. coli* S17-1 were transformed with plasmid pKKB60.6 or pSOB3 (derivatives of suicide vector pAKE600) to create the donor strain, and the WT *P. aeruginosa* PAO1161 Rif^R was used as the recipient. The allele exchange procedure was performed as described previously [64]. The verification of the allele exchange was performed with PCR.

4.2. Motility and Biofilm Formation Assays

Motility assays were performed as described previously using cultures in an LB medium [65]. To standardize the assay, all plates contained the same volume of the medium. The biofilm amount was measured with the crystal violet staining method [66].

4.3. Protein Purification

The *E. coli* BL21(DE3) strains transformed with pKKB28.3 or pMEB265 encoding a His₆-PA3973 or PA3973-His₆ fusion, respectively, were grown to exponential phase in an LB medium with the supplementation of 0.5 mM IPTG. The cells were harvested with

centrifugation, resuspended in a LEW buffer [50 mM sodium phosphate buffer, pH 8.0; 300 mM NaCl] supplemented with lysozyme (1 mg/mL), PMSF (1 mM), and benzonase nuclease (250 U, Sigma), and sonicated. His₆-tagged proteins were purified from the cell lysate using chromatography on Ni-agarose columns (Protino Ni-TED 1000, Macherey-Nagel, Düren, Germany) with 300 mM imidazole in LEW buffer used for elution. The purification procedure was monitored by SDS-PAGE using a Pharmacia PHAST gel system. The fractions containing the purified protein were dialyzed overnight in 50 mM Tris-HCl buffer (pH 8.0) containing 5% (*v/v*) glycerol and stored in aliquots at -80°C .

4.4. Cross-Linking of Purified Protein

The purified His₆-PA3973 was cross-linked with increasing concentrations of glutaraldehyde as previously described [67]. Samples were then suspended in the loading buffer [50 mM Tris-HCl (pH 8.0), 0.1 M DTT, 2% SDS, 0.1% bromophenol blue, 10% glycerol], boiled, and separated on an SDS-PAGE gel, transferred to nitrocellulose membrane (Amersham Protran, Cytiva, Germany), and used in a Western blot analysis with the use of anti-His₆ antibodies.

4.5. RNA Isolation, RNA-Seq

The total RNA was isolated from three independent replicate samples of *P. aeruginosa* PAO1161 overexpressing the PA3973 gene, samples of control strain carrying the empty vector, as well as *P. aeruginosa* PAO1161 WT and Δ PA3973 strain. RNA isolation, sequencing, as well as data analysis were performed essentially as described previously [68]. The raw data is available in the NCBI's Gene Expression Omnibus (GEO) database (<http://www.ncbi.nlm.nih.gov/geo/>) under accession number GSE211771 (released 22 November 2022).

4.6. RT-qPCR Analyses

For the qRT-PCR analyses, cells from the PAO1161 pKKB3.11 (*lacI^q-tacp-PA3973*) and PAO1161 pAMB9.37 (*lacI^q-tacp*) strains grown in a selective LB medium supplemented with 0.05 mM IPTG, or from PAO1161 WT and Δ PA3973 mutant cultures grown in the rich medium were collected from 2 mL of cultures at an optical density at 600 nm 0.5. For the testing influence of stress conditions on the expression of selected genes, the RNA was isolated from the WT PAO1161 cultures grown in a rich medium supplemented with subinhibitory concentrations of carbenicillin (32 $\mu\text{g}/\text{mL}$), kanamycin (10 $\mu\text{g}/\text{mL}$), tetracycline (4 $\mu\text{g}/\text{mL}$), or hydroxylamine at concentration 50 $\mu\text{g}/\text{mL}$. The RNA was isolated from 2 mL of cultures collected at an optical density at 600 nm 0.5.

Three biological replicates of total RNA (2 μg per reaction) from each strain served as a template for cDNA synthesis with TranScriba Kit (A&A Biotechnology, Gdansk, Poland). The cDNA was used as a template in qPCR performed with 5xHOT FIREPol EvaGreen qPCR Mix Plus (Solis Biodyne, Tartu, Estonia). Three technical replicates per each gene/sample were used. The sequences of primers used for RT-qPCR analysis are listed in Table S2. The efficiency of the quantitative PCR reaction with each primer pair was calculated and used to calculate the ratio of each studied gene to the reference gene. All primer pairs used showed the efficiency of amplification between 0.95–1.05. Changes in individual gene expression between the mutant and WT strain, between PA3973 over-producer and control strain, or between treated and untreated cells were calculated with the normalization of C_p values to mean C_p value for a *proC* (PA0393) reference gene using the Pfaffl method [69]. The qPCR was performed using the Light Cycler 480 (Roche). PCR products were detected with SYBR green fluorescent dye and amplified according to the following protocol: one cycle at 95°C for 15 min followed by 40 cycles at 95°C for 15 s and 60°C for 20 s. Each 18 μL reaction contained 3.6 μL 5 \times reaction mix, 1 μL of five times diluted cDNA, and 1.5 μL of mixed 6 μM primers. In each run, negative controls (no cDNA) for each primer set were included.

4.7. Chromatin Immunoprecipitation and Sequencing

The ChIP-seq was performed as previously [68]. *P. aeruginosa* Δ PA3973 strain carrying pMEB255 (*tacp-PA3973-flag*) or pABB28.1 (*tacp-flag*) vectors were grown in rich medium containing chloramphenicol (75 μ g/mL) and 0.05 mM IPTG as the inducer. The ChIP procedure was performed using anti-FLAG antibodies (MA1-91878, Invitrogen). Data were processed essentially as previously [68]. The sequencing data is available in the NCBI's Gene Expression Omnibus (GEO) database (<http://www.ncbi.nlm.nih.gov/geo/>) under accession number GSE211769 (released 22 November 2022).

4.8. In Vitro Protein-DNA Interactions

The electrophoretic mobility shift assay with purified PCR products (~100 ng in reaction) and PA3973-His₆ was conducted in a binding buffer [10 mM Tris-HCl (pH 8.5), 10 mM MgCl₂, 100 mM KCl, 0.1 mg/mL BSA]. The tested DNA fragments were amplified using the appropriate pair of primers listed in Table S2: #13/#4 for PA3973p; #13/#14 for PA3973p*; #15/#16 for PA0061p; #17/#18 for PA0195p; #19/#20 for PA2468p; #21/#22 for PA2722p; #23/#24 for PA4156p; #25/#26 for PA4710p. Approximately 300 ng of competitor DNA fragment, obtained by the annealing of oligonucleotides #27/#28 (Table S2), was used as an internal control in each reaction. The DNA fragments were incubated in a binding buffer with the increasing concentration of purified PA3973-His₆ at 23 °C for 30 min. All reactions were prepared in a total volume of 20 μ L. The complexes were separated on a 1.5% agarose gel in 0.5 \times Tris-borate-EDTA (TBE) buffer at 4 °C. The DNA was stained with ethidium bromide and visualized under UV light.

4.9. Regulatory Experiments with Promoter-*xylE* Fusions in *E. coli*

The *E. coli* DH5 α double transformants carrying pPT01 derivatives with the promoter regions of selected *P. aeruginosa* genes fused to the *xylE* reporter gene plus pAMB9.37 (*tacp*) or pKKB3.11 (*tacp-PA3973*) were assayed for catechol 2,3-oxygenase activity (the activity of the product of *xylE*). The experiment was performed as previously described [70] using cell extracts prepared from exponentially growing cultures in LB. Measurements of the amount of the protein in extracts were conducted using the Bradford assay [71].

Supplementary Materials: The supporting information can be downloaded at: <https://www.mdpi.com/article/10.3390/ijms232314584/s1>. (see Refs. [4,68,72–81]).

Author Contributions: Conceptualization, A.A.B.; methodology, K.K., A.K., M.M.-B., J.G., K.Z., R.G., A.A.B.; software, A.K., K.K., M.M.-B., J.G., K.Z., R.G., A.A.B.; validation, K.K., A.K., M.M.-B., A.A.B.; formal analysis, K.K., A.K., M.M.-B., A.A.B.; investigation, K.K., A.K., M.M.-B., A.A.B.; resources, K.K., A.K., M.M.-B., J.G., K.Z., R.G., A.A.B.; data curation, K.K., A.K., M.M.-B., J.G., K.Z., R.G., A.A.B.; writing-original draft preparation, A.A.B., M.M.-B., A.K.; writing-review and editing, A.A.B., M.M.-B., A.K.; visualization, K.K., A.K., M.M.-B., A.A.B.; supervision, A.A.B.; project administration, A.A.B.; funding acquisition, A.A.B. All authors have read and agreed to the published version of the manuscript.

Funding: This research was funded by the National Science Centre in Poland (grant 2015/18/E/NZ2/00675).

Institutional Review Board Statement: Not applicable.

Informed Consent Statement: Not applicable.

Data Availability Statement: Sequencing data are available in the NCBI's Gene Expression Omnibus (GEO) database (<http://www.ncbi.nlm.nih.gov/geo/>) under accession number GSE211769 [ChIP-seq data] and GSE211771 [RNA-seq data] (released 22 November 2022).

Acknowledgments: We thank Szymon Owczarek, a graduate student at the Warsaw University of Technology, Faculty of Chemistry, Warsaw, Poland for the construction of vectors for PA3972-71 mutagenesis and preliminary studies on the characterization of PA3972-71 from *P. aeruginosa*. This work was supported by the National Science Centre in Poland (grant 2015/18/E/NZ2/00675). We acknowledge financial and technical support from the Institute of Biochemistry and Biophysics, Polish Academy of Sciences, Warsaw, Poland.

Conflicts of Interest: The authors declare no conflict of interest.

Appendix A

Table A1. List of the most enriched PA3973 bound sites identified in the *P. aeruginosa* PAO1161 genome (FE > 4). Abbreviations: P-promoter; T-terminator; gb-gene body; +/– strand in PAO1161 genome; FE-fold enrichment for ChIP-seq data; FC-fold change for RNA-seq data; NA-not annotated, genes identified only in PAO1161 strain but not in PAO1; PseudoCAP categories as in Figure 3B [11].

Peak Summit	FE	Feature	PAO1161 ID (D3C65_)	PAO1 ID	Product	FC PA3973+ vs. EV+	FC ΔPA3973 vs. WT	Pseudo CAP
1,062,605	17.78	T+	05115	PA3974	hybrid sensor histidine kinase/response regulator	0.77	1.00	TCRS
1,062,605	17.78	P+	05120	PA3973	TetR/AcrR family transcriptional regulator	111.53	0.01	TR
863,356	13.68	P–	04180	PA4157	IclR family transcriptional regulator	0.99	0.90	TR
863,356	13.68	P+	04185	PA4156	TonB-dependent receptor FvbA	0.91	0.99	TSM
5,408,527	11.95	P–	25685	PA4709	hemin-degrading factor PhuS	0.94	1.02	PE; TSM
5,408,527	11.95	P+	25690	PA4710	TonB-dependent hemoglobin/transferrin/lactoferrin family receptor PhuR	1.61	1.31	TSM
74,770	9.93	P–	00350	PA0061	hypothetical protein	0.55	0.99	HUU
74,770	9.93	T–	00355	PA0062	hypothetical protein	0.84	0.99	HUU
2,439,925	8.05	P–	11790	PA2722	GFA family protein	0.83	1.12	HUU
2,439,925	8.05	T–	11795	PA2721	VOC family protein	0.90	0.93	HUU
223,938	7.31	T+	01035	PA0194	TauD/TfdA family dioxygenase	1.14	1.07	PE
223,938	7.31	P+	01040	PA0195	Re/Si-specific NAD(P)(+) transhydrogenase subunit alpha (PntAA)	1.06	1.24	EM; TSM
2,728,908	7.02	T+	13155	PA2469	LysR family transcriptional regulator	0.86	0.99	TR
2,728,908	7.02	P+	13160	PA2468	ECF sigma factor FoxI	2.44	0.90	TR
5,817,693	6.44	T+	27515	PA5057	poly(3-hydroxyalkanoate) depolymerase PhaD	0.91	0.92	CCC
5,817,693	6.44	P+	27520	PA5058	class II poly(R)-hydroxyalkanoic acid synthase	0.73	1.14	CIM
5,358,006	6.44	T+	25450	NA	hypothetical protein PhaC	1.48	1.12	NA

Table A1. Cont.

Peak Summit	FE	Feature	PAO1161 ID (D3C65_)	PAO1 ID	Product	FC PA3973+ vs. EV+	FC ΔPA3973 vs. WT	Pseudo CAP
5,358,006	6.44	P+	25455	NA	serine/threonine-protein phosphatase	1.66	1.10	NA
1,536,054	6.29	P−	07345	PA3552	UDP-4-amino-4-deoxy-L-arabinose-oxoglutarate aminotransferase ArnB	1.31	1.00	AP; ARS; CWLC
1,536,054	6.29	T−	07350	PA3551	alginate biosynthesis protein AlgA	1.06	1.05	AP; SF; CWLC
1,229,065	6.17	T+	05895	PA3829	alpha/beta hydrolase	0.59	0.94	HUU
1,229,065	6.17	P+	05900	PA3828	LPS export ABC transporter permease LptF	0.98	1.00	MP
2,863,600	5.27	T+	13525	PA2396	N(5)-hydroxyornithine transformylase PvdF	0.84	1.04	AP; SF
2,863,600	5.27	T−	13530	PA2395	formylglycine-generating enzyme family protein PvdO	1.01	0.86	AP
546,136	5.10	T+	02560	PA0484	ACT domain-containing protein	0.53	1.27	HUU
546,136	5.10	T−	02565	PA0485	EamA family transporter	0.73	1.04	MP
2,596,292	4.94	T+	12535	PA2583	response regulator	1.42	1.06	TCRS; TR
2,596,292	4.94	P+	12540	PA2582	ProQ activator of osmoprotectant transporter ProP	1.17	0.96	HUU
4,238,513	4.88	P−	19950	PA1178	PhoP/Q and low Mg ²⁺ inducible outer membrane protein H1	1.19	0.96	AP; MP; TSM
4,238,513	4.88	P+	19955	PA1177	periplasmic nitrate reductase NapE	0.43	1.41	EM
1,565,661	4.83	P−	07455	PA3531	Bacterioferritin BfrB	0.28	1.03	AP; TSM
1,565,661	4.83	T−	07460	PA3530	(2Fe-2S)-binding protein Bfd	6.48	0.63	HUU
4,782,429	4.71	P−	22665	PA0672	biliverdin-producing heme oxygenase HemO	0.91	1.08	BCPGC
4,782,429	4.71	P+	22670	PA0671	translesion DNA synthesis-associated protein ImuA	2.61	1.00	HUU
6,336,688	4.46	P−	29970	PA5523	aspartate aminotransferase family protein	0.80	0.99	PE
6,336,688	4.46	P+	29975	PA5524	SDR family oxidoreductase	0.83	0.98	PE
5,155,744	4.45	P−	24430	NA	site-specific integrase	1.53	1.10	NA
5,155,744	4.45	T−	24435	NA	hypothetical protein	3.05	1.18	NA
4,752,637	4.28	P−	22570	PA0691	Transposase PhdA		NA	HUU
4,752,637	4.28	T−	22575	PA0690	phosphate depletion regulated TPS partner A, PdtA	0.81	1.04	HUU

Table A1. Cont.

Peak Summit	FE	Feature	PAO1161 ID (D3C65_)	PAO1 ID	Product	FC PA3973+ vs. EV+	FC ΔPA3973 vs. WT	Pseudo CAP
1,495,167	4.28	T+	07140	PA3588	outer membrane porin, OprD	0.77	1.03	CCC; MP; TSM
1,495,167	4.28	T−	07145	PA3587	LysR family transcriptional regulator MetR	0.94	1.01	TR
2,454,141	4.23	T+	11865	PA2708	DUF748 domain-containing protein	0.80	0.96	HUU
2,454,141	4.23	P+	11870	PA2707	MoxR family ATPase	0.67	1.17	HUU
2,610,170	4.18	T+	12605	PA2570.1	tRNA-Leu	0.92	1.10	NCRNA
2,610,170	4.18	P+	12610	PA2570	PA-I galactophilic lectin LecA	1.17	1.44	AP; MA; CWLC
534,991	4.14	T+	02505	PA0473	glutathione S-transferase family protein PsfA	0.77	1.06	PE
534,991	4.14	P+	02510	PA0474	PaaI family thioesterase		0.99	HUU
2,138,915	4.09	P−	10205	PA3015	hypothetical protein	0.64	1.07	HUU
2,138,915	4.09	P+	10210	PA3014	fatty acid oxidation complex subunit alpha FadB	0.49	1.03	AABM; FAPM
559,247	4.07	P−	02635	PA0499	probable pili assembly chaperone	1.41	1.17	CHSP; MA
559,247	4.07	P+	02640	PA0500	biotin synthase BioB	1.07	1.01	BCPGC
5,632,780	4.02	P−	26750	PA4913	branched-chain amino acid ABC transporter substrate-binding protein	0.66	1.07	TSM
5,632,780	4.02	P+	26755	PA4914	LysR family transcriptional regulator AmaR	0.69	1.10	TR
1,186,255	4.00	P−	05685	PA3867	recombinase family protein	1.49	1.00	DRRMR
1,186,255	4.00	P+	05690	PA3866	pyocin protein S4	2.04	1.09	AP; SF
4,470,329	17.53	gb+	21130	PA0958	outer membrane porin OprD	0.70	1.00	TSM
977,796	10.14	gb+	04705	PA4056	riboflavin-specific deaminase/reductase RibD	0.96	0.94	BCPGC
1,833,017	8.32	gb+	08720	PA3290	DUF2235 domain-containing protein Tle1	1.50	1.05	SF
578,029	7.73	gb−	02735	PA0518	cytochrome c551, NirM	0.04	1.34	BCPGC; EM
3,067,087	7.41	gb+	14395	PA2227	AraC-type transcriptional regulator VqsM	1.62	1.22	TR
6,269,947	6.38	gb+	29640	PA5459	class I SAM-dependent methyltransferase	1.47	0.87	CWLC
4,031,730	6.26	gb−	18950	PA1369	hypothetical protein	1.20	1.29	HUU
5,431,668	6.05	gb+	25790	PA4729	3-methyl-2-oxobutanoate hydroxymethyltransferase PanB	0.74	0.97	BCPGC

Table A1. Cont.

Peak Summit	FE	Feature	PAO1161 ID (D3C65_)	PAO1 ID	Product	FC PA3973+ vs. EV+	FC Δ PA3973 vs. WT	Pseudo CAP
3,604,758	5.72	gb+	16880	PA1766	alpha-L-glutamate ligase-like protein	1.49	1.00	HUU
2,690,883	5.55	gb+	12965	PA2507	catechol 1,2-dioxygenase CatA	0.72	1.21	CCC
4,554,008	4.92	gb−	21565	PA0879	acyl-CoA dehydrogenase	0.64	1.00	PE
2,637,920	4.47	gb+	12745	PA2546	ring-cleaving dioxygenase	0.83	0.98	PE
4,271,470	4.45	gb−	20110	PA1150	pyocin-S2, Pys2	1.57	1.12	AP; SF
2,759,466	4.44	gb−	13220	PA2456	hypothetical protein	1.48	1.32	HUU
4,010,081	4.38	gb−	18870	PA1385	glycosyltransferase family 1 protein	1.96	1.21	CWLC
126,634	4.28	gb−	00565	NA	hypothetical protein	0.92	1.12	NA
4,014,784	4.27	gb−	18885	PA1382	type II secretion system protein GspD	0.82	1.20	PSE
4,338,596	4.21	gb−	20435	PA1089	HAD family hydrolase	1.98	0.91	HUU
801,087	4.21	gb−	03900	PA4211	phenazine biosynthesis protein PhzB 1	1.75	1.17	SF
1,194,762	4.20	gb−	05725	NA	hypothetical protein		1.55	NA
1,983,113	4.18	gb+	09485	PA3148	UDP-N-acetylglucosamine 2-epimerase WbpI	1.58	1.11	CWLC; PE
3,666,357	4.11	gb−	17215	PA1702	type III secretion protein Pcr4		0.81	PSE; SF
2,377,635	4.06	gb−	11420	PA2780	bacterial swarming regulator BswR	1.27	1.08	TR
3,419,943	4.04	gb+	16040	PA1920	class III (anaerobic) ribonucleoside-triphosphate reductase subunit NrdD	0.06	2.91	NBM
4,011,617	4.04	gb−	18875	PA1384	UDP-glucose 4-epimerase Gale	1.58	1.12	CCC; CIM; NBM

Table A2. List of 38 genes altered in response to PA3973 excess with PA3973 binding site in their promoter regions or adjacent to these genes. Full data for each peak/gene could be found in Tables S3–S6. Abbreviations: P-promoter; T-terminator; gb-gene body; +/− strand in PAO1161 genome; FE-fold enrichment for ChIP-seq data; FC-fold change for RNA-seq data; NA-not annotated, genes identified only in PAO1161 strain but not in PAO1; PseudoCAP categories as in Figure 3B [11].

Peak Summit	ChIP-Seq				Product	RNA-Seq (FC)		Pseudo CAP
	FE	Feature	PAO1161_ID	PAO1_ID		PA3973+ vs. EV+	Δ PA3973 vs. WT	
1,062,605	17.8	P+	D3C65_05120	PA3973	TetR/AcrR family transcriptional regulator	111.53	0.01	TR
1,565,661	4.8	T−	D3C65_07460	PA3530	(2Fe-2S)-binding protein	6.48	0.63	HUU
2,793,777	2.3	P−	D3C65_13380	PA2426	RNA polymerase factor sigma-70	5.52	0.97	TR
5,055,569	2.3	P+	D3C65_23920	PA4515	PKHD-type hydroxylase	4.87	0.89	HUU

Table A2. Cont.

Peak Summit	ChIP-Seq				Product	RNA-Seq (FC)		
	FE	Feature	PAO1161_ID	PAO1_ID		PA3973+ vs. EV+	ΔPA3973 vs. WT	Pseudo CAP
6,162,338	2.7	P−	D3C65_29150	PA5369.2	23S ribosomal RNA	4.05	ND	NCRNA
5,386,852	3.0	P−	D3C65_25575	PA4690.2	23S ribosomal RNA	4.04	ND	NCRNA
4,791,422	3.0	P−	D3C65_22690	NA	23S ribosomal RNA	3.98	ND	NA
4,726,925	2.8	T−	D3C65_22440	PA0716	ATP-binding cassette domain-containing protein	3.85	1.17	HUU
723,925	2.9	P+	D3C65_03525	NA	23S ribosomal RNA	3.76	ND	NA
1,148,582	2.3	P−	D3C65_05510	PA3899	sigma-70 family RNA polymerase sigma factor	3.71	0.91	TR
5,300,300	2.5	P−	D3C65_25120	PA4625	filamentous hemagglutinin N-terminal domain	3.46	0.93	CWLC; SF
5,155,744	4.5	T−	D3C65_24435	NA	hypothetical protein	3.05	1.18	NA
4,447,533	3.8	P+	D3C65_20980	PA0985	pyocin S5	2.82	1.11	MP; SF
4,782,429	4.7	P+	D3C65_22670	PA0671	translesion DNA synthesis-associated protein ImuA	2.61	1.00	HUU
1,966,031	2.9	P+	D3C65_09410	PA3162	30S ribosomal protein S1	2.54	1.04	TPTMD
2,728,908	7.0	P+	D3C65_13160	PA2468	ECF sigma factor FoxI	2.44	0.90	TR
883,435	2.2	T−	D3C65_04265	PA4140	FAD-binding protein	2.35	0.96	HUU
5,055,569	2.3	P−	D3C65_23915	PA4514	TonB-dependent siderophore receptor	2.19	1.31	TSM
4,729,931	2.3	P−	D3C65_22445	PA0715	RNA-directed DNA polymerase	2.14	1.17	RPTP
6,345,389	3.5	P−	D3C65_30010	PA5531	protein TonB	2.11	0.98	TSM
2,754,299	2.9	P+	D3C65_13195	PA2461	pentapeptide repeat-containing protein	2.09	1.15	HUU
1,186,255	4.0	P+	D3C65_05690	PA3866	pyocin protein	2.04	1.09	AP; SF
6,171,043	2.0	P+	D3C65_29200	PA5375	BCCT family transporter	0.49	0.93	MP; TSM
2,138,915	4.1	P+	D3C65_10210	PA3014	fatty acid oxidation complex subunit alpha FadB	0.49	1.03	AABM; FAPM
4,836,775	2.7	T+	D3C65_22855	PA4309	methyl-accepting chemotaxis protein PctA	0.47	1.04	AP; CHE
1,659,181	2.6	T−	D3C65_07870	PA3451	hypothetical protein	0.44	1.07	HUU
2,101,587	2.3	P−	D3C65_10015	PA3049	ribosome modulation factor	0.44	1.36	TPTMD
4,238,513	4.9	P+	D3C65_19955	PA1177	periplasmic nitrate reductase NapE protein	0.43	1.41	EM
5,605,641	2.1	P−	D3C65_26630	PA4889	ferredoxin reductase	0.43	0.72	PE
141,900	3.3	T+	D3C65_00655	PA0121	GntR family transcriptional regulator	0.40	0.91	HUU

Table A2. Cont.

Peak Summit	ChIP-Seq					RNA-Seq (FC)		
	FE	Feature	PAO1161_ID	PAO1_ID	Product	PA3973+ vs. EV+	ΔPA3973 vs. WT	Pseudo CAP
4,782,429	3.1	P+	D3C65_00220	NA	transposase	0.39	1.56	NA
1,724,552	2.2	P+	D3C65_08220	PA3384	phosphonate ABC transporter ATP-binding protein	0.37	ND	TSM
1,300,584	2.2	P+	D3C65_06250	PA3762	NGG1p interacting factor NIF3	0.35	1.17	HUU
3,815,440	2.1	P+	D3C65_17955	PA1561	PAS domain S-box protein	0.34	1.31	AP; CHE
3,027,948	2.8	P−	D3C65_14225	PA2259	LacI family DNA-binding transcriptional regulator	0.33	1.06	TR
1,565,661	4.8	P−	D3C65_07455	PA3531	Bacterioferritin (Bfr)	0.28	1.03	AP; TSM
4,729,931	2.3	T−	D3C65_22450	PA0714	hypothetical protein	0.26	1.16	HUU
3,690,709	2.7	P−	D3C65_17365	PA1673	hemerythrin	0.20	1.52	HUU

References

- Gales, A.C.; Jones, R.N.; Turnidge, J.; Rennie, R.; Ramphal, R. Characterization of *Pseudomonas Aeruginosa* Isolates: Occurrence Rates, Antimicrobial Susceptibility Patterns, and Molecular Typing in the Global SENTRY Antimicrobial Surveillance Program, 1997-1999. *Clin. Infect Dis.* **2001**, *32* (Suppl. 2), S146–S155. [\[CrossRef\]](#) [\[PubMed\]](#)
- Lansbury, L.; Lim, B.; Baskaran, V.; Lim, W.S. Co-Infections in People with COVID-19: A Systematic Review and Meta-Analysis. *J. Infect.* **2020**, *81*, 266–275. [\[CrossRef\]](#) [\[PubMed\]](#)
- Parkins, M.D.; Somayaji, R.; Waters, V.J. Epidemiology, Biology, and Impact of Clonal *Pseudomonas aeruginosa* Infections in Cystic Fibrosis. *Clin. Microbiol. Rev.* **2018**, *31*, e00019-18. [\[CrossRef\]](#) [\[PubMed\]](#)
- Modrzejewska, M.; Kawalek, A.; Bartosik, A.A. The LysR-type transcriptional regulator BsrA (PA2121) controls vital metabolic pathways in *Pseudomonas aeruginosa*. *mSystems* **2021**, *6*, e0001521. [\[CrossRef\]](#) [\[PubMed\]](#)
- Poole, K. Stress responses as determinants of antimicrobial resistance in *Pseudomonas aeruginosa*: Multidrug efflux and more. *Can J. Microbiol.* **2014**, *60*, 783–791. [\[CrossRef\]](#)
- Udaondo, Z.; Ramos, J.-L.; Segura, A.; Krell, T.; Daddaoua, A. Regulation of carbohydrate degradation pathways in *Pseudomonas* involves a versatile set of transcriptional regulators. *Microb. Biotechnol.* **2018**, *11*, 442–454. [\[CrossRef\]](#)
- Soukari, F.; Williams, P.; Stocks, M.J.; Cámara, M. *Pseudomonas aeruginosa* Quorum Sensing systems as drug discovery targets: Current Position and Future Perspectives. *J. Med. Chem.* **2018**, *61*, 10385–10402. [\[CrossRef\]](#)
- Bartosik, A.A.; Glabski, K.; Jecz, P.; Mikulska, S.; Fogtman, A.; Kobłowska, M.; Jagura-Burdzy, G. Transcriptional profiling of *parA* and *parB* mutants in actively dividing cells of an opportunistic human pathogen *Pseudomonas aeruginosa*. *PLoS ONE* **2014**, *9*, e87276. [\[CrossRef\]](#)
- Galán-Vásquez, E.; Luna, B.; Martínez-Antonio, A. The regulatory network of *Pseudomonas aeruginosa*. *Microb. Inform. Exp.* **2011**, *1*, 3. [\[CrossRef\]](#)
- Stover, C.K.; Pham, X.Q.; Erwin, A.L.; Mizoguchi, S.D.; Warren, P.; Hickey, M.J.; Brinkman, F.S.; Hufnagle, W.O.; Kowalik, D.J.; Lagrou, M.; et al. Complete genome sequence of *Pseudomonas aeruginosa* PAO1, an opportunistic pathogen. *Nature* **2000**, *406*, 959–964. [\[CrossRef\]](#)
- Winsor, G.L.; Griffiths, E.J.; Lo, R.; Dhillon, B.K.; Shay, J.A.; Brinkman, F.S.L. Enhanced annotations and features for comparing thousands of *Pseudomonas* genomes in the pseudomonas genome database. *Nucleic Acids Res.* **2016**, *44*, D646–D653. [\[CrossRef\]](#)
- Balasubramanian, D.; Schnepfer, L.; Kumari, H.; Mathee, K. A dynamic and intricate regulatory network determines *Pseudomonas aeruginosa* virulence. *Nucleic Acids Res.* **2013**, *41*, 1–20. [\[CrossRef\]](#)
- Huang, H.; Shao, X.; Xie, Y.; Wang, T.; Zhang, Y.; Wang, X.; Deng, X. An integrated genomic regulatory network of virulence-related transcriptional factors in *Pseudomonas aeruginosa*. *Nat. Commun.* **2019**, *10*, 2931. [\[CrossRef\]](#)
- Ramos, J.L.; Martínez-Bueno, M.; Molina-Henares, A.J.; Terán, W.; Watanabe, K.; Zhang, X.; Gallegos, M.T.; Brennan, R.; Tobes, R. The TetR family of transcriptional repressors. *Microbiol. Mol. Biol. Rev.* **2005**, *69*, 326–356. [\[CrossRef\]](#)
- Deng, W.; Li, C.; Xie, J. The Underling mechanism of bacterial TetR/AcrR family transcriptional repressors. *Cell Signal.* **2013**, *25*, 1608–1613. [\[CrossRef\]](#)

16. Aramaki, H.; Yagi, N.; Suzuki, M. Residues important for the function of a multihelical dna binding domain in the new transcription factor family of cam and Tet repressors. *Protein. Eng.* **1995**, *8*, 1259–1266. [[CrossRef](#)]
17. Engohang-Ndong, J.; Baillat, D.; Aumercier, M.; Bellefontaine, F.; Besra, G.S.; Loch, C.; Baulard, A.R. EthR, a repressor of the TetR/CamR family implicated in ethionamide resistance in *Mycobacteria*, octamerizes cooperatively on its operator. *Mol. Microbiol.* **2004**, *51*, 175–188. [[CrossRef](#)]
18. Orth, P.; Schnappinger, D.; Hillen, W.; Saenger, W.; Hinrichs, W. Structural basis of gene regulation by the tetracycline inducible Tet Repressor-Operator system. *Nat. Struct. Biol.* **2000**, *7*, 215–219. [[CrossRef](#)]
19. Schumacher, M.A.; Miller, M.C.; Grkovic, S.; Brown, M.H.; Skurray, R.A.; Brennan, R.G. Structural mechanisms of QacR induction and multidrug recognition. *Science* **2001**, *294*, 2158–2163. [[CrossRef](#)]
20. Kisker, C.; Hinrichs, W.; Tovar, K.; Hillen, W.; Saenger, W. The complex formed between Tet repressor and tetracycline-Mg²⁺ reveals mechanism of antibiotic resistance. *J. Mol. Biol.* **1995**, *247*, 260–280. [[CrossRef](#)]
21. Su, C.-C.; Rutherford, D.J.; Yu, E.W. Characterization of the multidrug efflux regulator AcrR from *Escherichia coli*. *Biochem Biophys. Res. Commun.* **2007**, *361*, 85–90. [[CrossRef](#)] [[PubMed](#)]
22. Ruiz, C.; Levy, S.B. Regulation of AcrAB expression by cellular metabolites in *Escherichia coli*. *J. Antimicrob. Chemother.* **2014**, *69*, 390–399. [[CrossRef](#)] [[PubMed](#)]
23. Grkovic, S.; Brown, M.H.; Skurray, R.A. Regulation of bacterial drug export systems. *Microbiol. Mol. Biol. Rev.* **2002**, *66*, 671–701. [[CrossRef](#)]
24. Aires, J.R.; Köhler, T.; Nikaido, H.; Plésiat, P. Involvement of an active efflux system in the natural resistance of *Pseudomonas aeruginosa* to aminoglycosides. *Antimicrob. Agents Chemother.* **1999**, *43*, 2624–2628. [[CrossRef](#)] [[PubMed](#)]
25. Matsuo, Y.; Eda, S.; Gotoh, N.; Yoshihara, E.; Nakae, T. MexZ-mediated regulation of MexXY multidrug efflux pump expression in *Pseudomonas aeruginosa* by binding on the *mexZ-mexX* intergenic DNA. *FEMS Microbiol. Lett.* **2004**, *238*, 23–28. [[CrossRef](#)]
26. Yamamoto, M.; Ueda, A.; Kudo, M.; Matsuo, Y.; Fukushima, J.; Nakae, T.; Kaneko, T.; Ishigatsubo, Y. Role of MexZ and PA5471 in Transcriptional regulation of MexXY in *Pseudomonas aeruginosa*. *Microbiol. (Read.)* **2009**, *155*, 3312–3321. [[CrossRef](#)]
27. Dean, C.R.; Visalli, M.A.; Projan, S.J.; Sum, P.-E.; Bradford, P.A. Efflux-mediated resistance to tigecycline (GAR-936) in *Pseudomonas aeruginosa* PAO1. *Antimicrob. Agents Chemother.* **2003**, *47*, 972–978. [[CrossRef](#)]
28. Fraud, S.; Poole, K. Oxidative stress induction of the MexXY multidrug efflux genes and promotion of aminoglycoside resistance development in *Pseudomonas aeruginosa*. *Antimicrob. Agents Chemother.* **2011**, *55*, 1068–1074. [[CrossRef](#)]
29. Lau, C.H.-F.; Fraud, S.; Jones, M.; Peterson, S.N.; Poole, K. Reduced Expression of the RplU-RpmA ribosomal protein operon in MexXY-Expressing pan-aminoglycoside-resistant mutants of *Pseudomonas aeruginosa*. *Antimicrob. Agents Chemother.* **2012**, *56*, 5171–5179. [[CrossRef](#)]
30. Masuda, N.; Sakagawa, E.; Ohya, S.; Gotoh, N.; Tsujimoto, H.; Nishino, T. Contribution of the MexX-MexY-OprM efflux system to intrinsic resistance in *Pseudomonas aeruginosa*. *Antimicrob. Agents Chemother.* **2000**, *44*, 2242–2246. [[CrossRef](#)]
31. Morita, Y.; Gilmour, C.; Metcalf, D.; Poole, K. Translational control of the antibiotic inducibility of the PA5471 gene required for MexXY multidrug efflux gene expression in *Pseudomonas aeruginosa*. *J. Bacteriol.* **2009**, *191*, 4966–4975. [[CrossRef](#)]
32. Morita, Y.; Sobel, M.L.; Poole, K. Antibiotic inducibility of the MexXY multidrug efflux system of *Pseudomonas aeruginosa*: Involvement of the antibiotic-inducible PA5471 gene product. *J. Bacteriol.* **2006**, *188*, 1847–1855. [[CrossRef](#)]
33. Kawalek, A.; Modrzejewska, M.; Zieniuk, B.; Bartosik, A.A.; Jagura-Burdzy, G. Interaction of ArmZ with the DNA-binding domain of MexZ induces expression of *mexXY* multidrug efflux pump genes and antimicrobial resistance in *Pseudomonas aeruginosa*. *Antimicrob. Agents Chemother.* **2019**, *63*, e01199-19. [[CrossRef](#)]
34. Bahl, C.D.; MacEachran, D.P.; O’Toole, G.A.; Madden, D.R. Purification, crystallization and preliminary x-ray diffraction analysis of Cif, a virulence factor secreted by *Pseudomonas aeruginosa*. *Acta Crystallogr. Sect. F Struct. Biol. Cryst. Commun.* **2010**, *66*, 26–28. [[CrossRef](#)]
35. MacEachran, D.P.; Stanton, B.A.; O’Toole, G.A. Cif is negatively regulated by the TetR family repressor CifR. *Infect Immun.* **2008**, *76*, 3197–3206. [[CrossRef](#)]
36. Chen, L.; Xu, X.; Fan, C.; Zhang, R.; Ji, Y.; Yu, Z.; Qu, H.; Feng, Z.; Chi, X.; Cheng, S.; et al. Pip serves as an intermediate in RpoS-modulated Phz2 expression and pyocyanin production in *Pseudomonas aeruginosa*. *Microb. Pathog.* **2020**, *147*, 104409. [[CrossRef](#)]
37. Hwang, S.; Kim, C.Y.; Ji, S.-G.; Go, J.; Kim, H.; Yang, S.; Kim, H.J.; Cho, A.; Yoon, S.S.; Lee, I. Network-assisted investigation of virulence and antibiotic-resistance systems in *Pseudomonas aeruginosa*. *Sci. Rep.* **2016**, *6*, 26223. [[CrossRef](#)]
38. Dong, Y.-H.; Zhang, X.-F.; Xu, J.-L.; Tan, A.-T.; Zhang, L.-H. VqsM, a novel AraC-type global regulator of quorum-sensing signalling and virulence in *Pseudomonas aeruginosa*. *Mol. Microbiol.* **2005**, *58*, 552–564. [[CrossRef](#)]
39. Kawalek, A.; Bartosik, A.A.; Glabski, K.; Jagura-Burdzy, G. *Pseudomonas aeruginosa* partitioning protein ParB acts as a nucleoid-associated protein binding to multiple copies of a *pars*-related motif. *Nucleic Acids Res.* **2018**, *46*, 4592–4606. [[CrossRef](#)]
40. Mirdita, M.; Schütze, K.; Moriawaki, Y.; Heo, L.; Ovchinnikov, S.; Steinegger, M. ColabFold: Making protein folding accessible to all. *Nat. Methods* **2022**, *19*, 679–682. [[CrossRef](#)]
41. Yan, Y.; Tao, H.; He, J.; Huang, S.-Y. The HDock server for integrated protein-protein docking. *Nat. Protoc.* **2020**, *15*, 1829–1852. [[CrossRef](#)] [[PubMed](#)]
42. Machanick, P.; Bailey, T.L. MEME-ChIP: Motif analysis of large dna datasets. *Bioinformatics* **2011**, *27*, 1696–1697. [[CrossRef](#)] [[PubMed](#)]

43. Elias, S.; Degtyar, E.; Banin, E. FvbA is required for vibriobactin utilization in *Pseudomonas aeruginosa*. *Microbiol. (Read.)* **2011**, *157*, 2172–2180. [[CrossRef](#)]
44. Mettrick, K.A.; Lamont, I.L. Different roles for anti-sigma factors in siderophore signalling pathways of *Pseudomonas aeruginosa*. *Mol. Microbiol.* **2009**, *74*, 1257–1271. [[CrossRef](#)] [[PubMed](#)]
45. Dotreppe, D.; Mullier, C.; Letesson, J.-J.; De Bolle, X. The alkylation response protein AidB is localized at the new poles and constriction sites in *Brucella abortus*. *BMC Microbiol.* **2011**, *11*, 257. [[CrossRef](#)]
46. Landini, P.; Hajec, L.I.; Volkert, M.R. Structure and transcriptional regulation of the *Escherichia coli* adaptive response gene AidB. *J. Bacteriol.* **1994**, *176*, 6583–6589. [[CrossRef](#)]
47. Mulrooney, S.B.; Howard, M.J.; Hausinger, R.P. The *Escherichia coli* alkylation response protein AidB is a redox partner of flavodoxin and binds RNA and acyl carrier protein. *Arch. Biochem. Biophys.* **2011**, *513*, 81–86. [[CrossRef](#)]
48. Hamill, M.J.; Jost, M.; Wong, C.; Elliott, S.J.; Drennan, C.L. Flavin-induced oligomerization in *Escherichia coli* adaptive response protein AidB. *Biochemistry* **2011**, *50*, 10159–10169. [[CrossRef](#)]
49. Mielecki, D.; Wrzesiński, M.; Grzesiuk, E. Inducible repair of alkylated DNA in microorganisms. *Mutat. Res. Rev. Mutat. Res.* **2015**, *763*, 294–305. [[CrossRef](#)]
50. Chang, W.; Small, D.A.; Toghrol, F.; Bentley, W.E. Microarray analysis of *Pseudomonas aeruginosa* reveals induction of pyocin genes in response to hydrogen peroxide. *BMC Genom.* **2005**, *6*, 115. [[CrossRef](#)]
51. Ferrández, A.; García, J.L.; Diaz, E. Transcriptional regulation of the divergent paa catabolic operons for phenylacetic acid degradation in *Escherichia coli*. *J. Biol. Chem.* **2000**, *275*, 12214–12222. [[CrossRef](#)]
52. Busby, S.; Irani, M.; Crombrugghe, B. Isolation of mutant promoters in the *Escherichia coli* galactose operon using local mutagenesis on cloned dna fragments. *J. Mol. Biol.* **1982**, *154*, 197–209. [[CrossRef](#)]
53. Wozniak, K.J.; Simmons, L.A. Hydroxyurea induces a stress response that alters dna replication and nucleotide metabolism in *Bacillus subtilis*. *J. Bacteriol.* **2021**, *203*, e0017121. [[CrossRef](#)]
54. Wade, J.T.; Struhl, K.; Busby, S.J.W.; Grainger, D.C. Genomic analysis of protein-dna interactions in bacteria: Insights into transcription and chromosome organization. *Mol. Microbiol.* **2007**, *65*, 21–26. [[CrossRef](#)]
55. Shimada, T.; Ishihama, A.; Busby, S.J.W.; Grainger, D.C. The *Escherichia coli* RutR transcription factor binds at targets within genes as well as intergenic regions. *Nucleic Acids Res.* **2008**, *36*, 3950–3955. [[CrossRef](#)]
56. Zhang, J.; Liu, B.; Gu, D.; Hao, Y.; Chen, M.; Ma, Y.; Zhou, X.; Reverter, D.; Zhang, Y.; Wang, Q. Binding site profiles and N-terminal minor groove interactions of the master quorum-sensing regulator LuxR enable flexible control of gene activation and repression. *Nucleic Acids Res.* **2021**, *49*, 3274–3293. [[CrossRef](#)]
57. Ochsner, U.A.; Vasil, A.I.; Vasil, M.L. Role of the Ferric Uptake Regulator of *Pseudomonas aeruginosa* in the regulation of siderophores and Exotoxin A expression: Purification and activity on iron-regulated promoters. *J. Bacteriol.* **1995**, *177*, 7194–7201. [[CrossRef](#)]
58. Sjöberg, B.-M.; Torrents, E. Shift in ribonucleotide reductase gene expression in *Pseudomonas aeruginosa* during infection. *Infect Immun.* **2011**, *79*, 2663–2669. [[CrossRef](#)]
59. Crespo, A.; Pedraz, L.; Torrents, E. Function of the *Pseudomonas aeruginosa* NrdR Transcription Factor: Global Transcriptomic Analysis and its role on ribonucleotide reductase gene expression. *PLoS ONE* **2015**, *10*, e0123571. [[CrossRef](#)]
60. Torrents, E. Ribonucleotide Reductases: Essential enzymes for bacterial life. *Front. Cell. Infect. Microbiol.* **2014**, *4*, 52. [[CrossRef](#)]
61. Neidhardt, F.C.; Bloch, P.L.; Smith, D.F. Culture medium for *Enterobacteria*. *J. Bacteriol.* **1974**, *119*, 736–747. [[CrossRef](#)] [[PubMed](#)]
62. Sambrook, J.; Fritsch, E.F.; Maniatis, T. *Molecular cloning. A Laboratory Manual*; Cold Spring Harbor Laboratory Press: New York, NY, USA, 1989.
63. Irani, V.R.; Rowe, J.J. Enhancement of transformation in *Pseudomonas aeruginosa* PAO1 by Mg²⁺ and heat. *BioTechniques* **1997**, *22*, 54–56. [[CrossRef](#)] [[PubMed](#)]
64. Lasocki, K.; Bartosik, A.A.; Mierzejewska, J.; Thomas, C.M.; Jagura-Burdzy, G. Deletion of the *parA* (*soj*) homologue in *Pseudomonas aeruginosa* causes ParB instability and affects growth rate, chromosome segregation, and motility. *J. Bacteriol.* **2007**, *189*, 5762–5772. [[CrossRef](#)] [[PubMed](#)]
65. Rashid, M.H.; Kornberg, A. Inorganic polyphosphate is needed for swimming, swarming, and twitching motilities of *Pseudomonas aeruginosa*. *Proc. Natl. Acad. Sci. USA* **2000**, *97*, 4885–4890. [[CrossRef](#)] [[PubMed](#)]
66. Djordjevic, D.; Wiedmann, M.; McLandsborough, L.A. Microtiter plate assay for assessment of listeria monocytogenes biofilm formation. *Appl. Environ. Microbiol.* **2002**, *68*, 2950–2958. [[CrossRef](#)]
67. Jagura-Burdzy, G.; Thomas, C.M. Purification of KorA protein from Broad Host Range plasmid RK2: Definition of a hierarchy of KorA operators. *J. Mol. Biol.* **1995**, *253*, 39–50. [[CrossRef](#)]
68. Kotecka, K.; Kawalek, A.; Kobylecki, K.; Bartosik, A.A. The AraC-type transcriptional regulator GliR (PA3027) activates genes of glycerolipid metabolism in *Pseudomonas aeruginosa*. *Int. J. Mol. Sci.* **2021**, *22*, 5066. [[CrossRef](#)]
69. Pfaffl, M.W. A New Mathematical Model for relative quantification in real-time RT-PCR. *Nucleic Acids Res.* **2001**, *29*, e45. [[CrossRef](#)]
70. Zukowski, M.M.; Gaffney, D.F.; Speck, D.; Kauffmann, M.; Findeli, A.; Wisecup, A.; Lecocq, J.P. Chromogenic identification of genetic regulatory signals in *Bacillus subtilis* based on expression of a cloned *Pseudomonas* gene. *Proc. Natl. Acad. Sci. USA* **1983**, *80*, 1101–1105. [[CrossRef](#)]
71. Bradford, M.M. A rapid and sensitive method for the quantitation of microgram quantities of protein utilizing the principle of protein-dye binding. *Anal. Biochem.* **1976**, *72*, 248–254. [[CrossRef](#)]

72. Hanahan, D. Studies on transformation of *Escherichia coli* with plasmids. *J. Mol. Biol.* **1983**, *166*, 557–580. [[CrossRef](#)]
73. Simon, R.; O'Connell, M.; Labes, M.; Pühler, A. Plasmid vectors for the genetic analysis and manipulation of *Rhizobium* and other Gram-negative bacteria. *Methods Enzymol.* **1986**, *118*, 640–659.
74. Bartosik, A.A.; Mierzejewska, J.; Thomas, C.M.; Jagura-Burdzy, G. ParB deficiency in *Pseudomonas aeruginosa* destabilizes the partner protein ParA and affects a variety of physiological parameters. *Microbiology* **2009**, *155*, 1080–1092. [[CrossRef](#)]
75. Kawalek, A.; Kotecka, K.; Modrzejewska, M.; Gawor, J.; Jagura-Burdzy, G.; Bartosik, A.A. Genome sequence of *Pseudomonas aeruginosa* PAO1161, a PAO1 derivative with the ICEPae1161 integrative and conjugative element. *BMC Genom.* **2020**, *21*, 14. [[CrossRef](#)]
76. Kovach, M.E.; Elzer, P.H.; Hill, D.S.; Robertson, G.T.; Farris, M.A.; Roop, R.M.; Peterson, K.M. Four new derivatives of the broad-host-range cloning vector pBBR1MCS, carrying different antibiotic-resistance cassettes. *Gene* **1995**, *166*, 175–176. [[CrossRef](#)]
77. Ludwiczak, M.; Dolowy, P.; Markowska, A.; Szarlak, J.; Kulinska, A.; Jagura-Burdzy, G. Global transcriptional regulator KorC coordinates expression of three backbone modules of the broad-host-range RA3 plasmid from IncU incompatibility group. *Plasmid* **2013**, *70*, 131–145. [[CrossRef](#)]
78. El-Sayed, A.K.; Hothersall, J.; Thomas, C.M. Quorum-sensing-dependent regulation of biosynthesis of the polyketide antibiotic mupirocin in *Pseudomonas fluorescens* NCIMB 10586. *Microbiology* **2001**, *147*, 2127–2139. [[CrossRef](#)]
79. Spratt, B.G.; Hedge, P.J.; te Heesen, S.; Edelman, A.; Broome-Smith, J.K. Kanamycin-resistant vectors that are analogues of plasmids pUC8, pUC9, pEMBL8 and pEMBL9. *Gene* **1986**, *41*, 337–342. [[CrossRef](#)]
80. Thorsted, P.B.; Shah, D.S.; Macartney, D.; Kostelidou, K.; Thomas, C.M. Conservation of the genetic switch between replication and transfer genes of IncP plasmids but divergence of the replication functions which are major host-range determinants. *Plasmid* **1996**, *36*, 95–111. [[CrossRef](#)]
81. Lukaszewicz, M.; Kostelidou, K.; Bartosik, A.A.; Cooke, G.D.; Thomas, C.M.; Jagura-Burdzy, G. Functional dissection of the ParB Homologue (KorB) from IncP-1 plasmid RK2. *Nucleic Acids Res.* **2002**, *30*, 1046–1055. [[CrossRef](#)]